

Simulation of Seismic Wave Propagation in Media with Complex Geometries

1 HEINER IGEL¹, MARTIN KÄSER¹, MARCO STUPAZZINI²
 2 ¹ Department of Earth and Environmental Sciences,
 3 Ludwig-Maximilians-University, Munich, Germany
 4 ² Department of Structural Engineering,
 5 Politecnico di Milano, Milano, Italy

6 Article Outline

7 Glossary
 8 Definition of the Subject
 9 Introduction
 10 The Evolution of Numerical Methods and Grids
 11 3D Wave Propagation on Hexahedral Grids:
 12 Soil-Structure Interactions
 13 3D Wave Propagation on Tetrahedral Grids:
 14 Application to Volcanology
 15 Local Time Stepping: Δt -Adaptation
 16 Discussion and Future Directions
 17 Acknowledgments
 18 Bibliography

19 Glossary

20 **Numerical methods** Processes in nature are often de-
 21 scribed by partial differential equations. Finding solu-
 22 tions to those equations is at the heart of many stud-
 23 ies aiming at the explanation of observed data. Sim-
 24 ulations of realistic physical processes requires gener-
 25 ally the use of numerical methods – a special branch
 26 of applied mathematics – that approximate the par-
 27 tial differential equations and allows solving them on
 28 computers. Examples are the finite-difference, finite-
 29 element, or finite-volume methods.

30 **Spectral elements** The spectral element method is an ex-
 31 tension of the finite element method that makes use
 32 of specific basis functions describing the solutions in-
 33 side each element. These basis functions (e. g., Cheby-
 34 shev or Legendre polynomials) allow the interpolation
 35 of functions exactly at certain collocation points. This
 36 is often termed spectral accuracy.

37 **Discontinuous Galerkin method** The discontinuous Gal-
 38 erkin method is a flavor of the finite-element method
 39 that allows discontinuous behavior of the spatial or
 40 temporal fields at the element boundaries. The discon-
 41 tinuities – that might be small in the case of continu-
 42 ous physical fields such as seismic waves – then define
 43 so-called Riemann problems that can be handled using

the concepts from finite-volume techniques. There-
 44 fore, the approximate solution is updated via numer-
 45 ical fluxes across the element boundaries.

Parallel algorithms All modern supercomputers make
 46 use of parallel architectures. This means that a large
 47 number of processors are performing (different) tasks
 48 on different data at the same time. Numerical algo-
 49 rithms need to be adapted to these hardware architec-
 50 tures by using specific programming paradigms (e. g.,
 51 the message passing interface MPI). The computa-
 52 tional efficiency of such algorithms strongly depends
 53 on the specific parallel nature of problem to be solved,
 54 and the requirement for inter-processor communica-
 55 tion.

Grid generation Most numerical methods are based on
 56 the calculation of the solutions at a large set of points
 57 (grids) that are either static or depend on time (adap-
 58 tive grids). These grids often need to be adapted to
 59 the specific geometrical properties of the objects to be
 60 modeled (volcano, reservoir, globe). Grids may be de-
 61 signed to follow domain boundaries and internal sur-
 62 faces. Before specific numerical solvers are employed
 63 the grid points are usually connected to form triangles
 64 or rectangles in 2D or hexahedra or tetrahedra in 3D.

68 Definition of the Subject

69 Seismology is the science that aims at understanding the
 70 Earth's interior and its seismic sources from measure-
 71 ments of vibrations of the solid Earth. The resulting im-
 72 ages of the physical properties of internal structures and
 73 the spatio-temporal behavior of earthquake rupture pro-
 74 cesses are prerequisites to understanding the dynamic evo-
 75 lution of our planet and the physics of earthquakes. One
 76 of the key ingredients to obtain these images is the calcu-
 77 lation of synthetic (or theoretical) seismograms for given
 78 earthquake sources and internal structures. These syn-
 79 thetic seismograms can then be compared quantitatively
 80 with observations and acceptable models be searched for
 81 using the theory of inverse problems. The methodologies
 82 to calculate synthetic seismograms have evolved dramati-
 83 cally over the past decades in parallel with the evolution of
 84 computational resources and the ever increasing volumes
 85 of permanent seismic observations in global, and regional
 86 seismic networks, volcano monitoring networks and ex-
 87 perimental campaigns. Today it is a tremendous challenge
 88 to extract an optimal amount of information from seismo-
 89 grams. The imaging process is still primarily carried out
 90 using ray theory or extensions thereof not fully taking into
 91 account the complex scattering processes that are occur-
 92 ring in nature.

Please note that the pagination is not final; in the print version an entry will in general not start on a new page.

To model seismic observations in their full complexity we need to be able to simulate wave propagation through 3D structures with constitutive relations that account for anisotropic elasticity, attenuation, porous media as well as complex internal interfaces such as layer boundaries or fault systems. This implies that numerical methods have to be employed that solve the underlying **partial differential equations** on computational grids. The high-frequency oscillatory nature of seismic wave fields makes this an expensive endeavor as far as computational resources are concerned. As seismic waves are propagating hundreds of wavelengths through scattering media, the required accuracy of the numerical approximations has to be of the highest possible order. Despite the fact that the physics of wave propagation is well understood, only recently computational algorithms are becoming available that allow us to accurately simulate wave propagation on many scale such as reservoirs, volcanoes, sedimentary basins, continents, and whole planets.

In addition to the **imaging** problem for subsurface structure and earthquake sources, the possibilities for 3D wave simulations has opened a new route to forecasting strong ground motions following large earthquakes in seismically active regions. In the absence of any hope to deterministically predict earthquakes, the calculation of earthquake scenarios in regions with sufficiently well known crustal structures and fault locations will play an important role in mitigating damage particularly due to potentially amplifying local velocity structures. However, to be able to employ the advanced 3D simulation technology in an efficient way, and to make use of the fast advance of supercomputing infrastructure, a paradigm shift in the concept of wave simulation software is necessary: The Earth science community has to build soft infrastructures that enable massive use of those simulation tools on the available high-performance computing infrastructure.

In this paper we want to present the state of the art of computational wave propagation and point to necessary developments in the coming years, particularly in connection with finding efficient ways to generate computational grids for models with complex topography, faults, and the combined simulation of soil and structures.

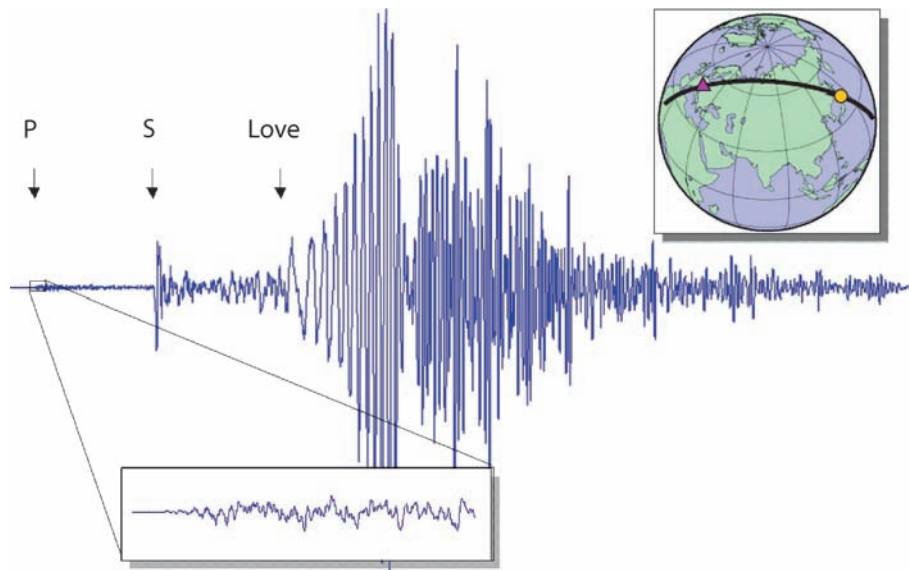
Introduction

We first illustrate the evolution of methodologies to calculate and model aspects of seismic observations for the case of global wave propagation. Seismology can look back at almost 50 years of systematic observations of earthquake induced teleseismic ground motions with the standardized global seismic and regional networks. The digital revolu-

tion in the past decades has altered the recording culture such that now seismometers are recording ground motions permanently rather than in trigger-mode, observations are becoming available in near-real time, and – because of the required sampling rates – the daily amount of observations automatically sent to the data centers is gigantic. If we take a qualitative look at a seismic observation (Fig. 1) we can illustrate what it takes to model either part or the whole information contained in such physical measurements.

In Fig. 1 a seismogram observed using a broadband seismometer (station WET in Germany) is shown. Globally observed seismograms following large earthquakes contain frequencies up to 1 Hz (P-wave motions) down to periods of around one hour (eigenmodes of the Earth) in which case modeling is carried out in the frequency domain. Seismograms of the kind shown in Fig. 1 contain many types of information. For large earthquakes the first part of the seismogram (inlet) contains valuable information on the spatio-temporal evolution of the earthquake rupture on a finite-size fault. A model of the fault slip history is a prerequisite to model the complete wave form of seismograms as the whole seismogram is affected by it unless severe low-pass filtering is applied. Information on the global seismic velocity structure is contained in the arrival times of numerous body-wave phases (here only P- and S-wave arrivals are indicated) and in the dispersive behavior of the surface waves (here the onset of the low-frequency Love waves is indicated). Further information is contained in the characteristics of the coda to body wave phases indicative of scattering in various parts of the Earth (see [62] for an account of modern observational seismology).

Adding a temporal and spatial scale to the above qualitative discussion reveals some important insight what it takes to simulate wave propagation on a planetary scale using grid-based numerical methods. Given the maximum frequency of around 1 Hz (P-waves) and 0.2 Hz (S-waves) the minimum wavelength in the Earth is expected to be $O(km)$, requiring $O(100\text{ m})$ type grid spacing at least in the crustal part of the Earth leading to $O(10^{12})$ necessary grid points (or volume elements) for accurate numerical simulations. This would lead to memory requirements $O(100\text{ TByte})$ that are today possible on some of the world's largest supercomputers. The message here is that despite the rapid evolution of computational power, the complete modeling of teleseismic observations using approaches such as spectral elements (e. g., [63,64]) requiring tremendous numbers of calculations to constrain structure and sources will remain a grand challenge for some time to come. However, in many cases it is not necessary or not even desirable to simulate or model the whole seis-



Simulation of Seismic Wave Propagation in Media with Complex Geometries, Figure 1

Transverse velocity seismogram of the M8.3 Tokachi-Oki earthquake near Hokkaido observed at station WET in Germany with a broadband seismometer. The total seismogram length is one hour. Arrival times of body wave phases (P, S) and the onset of transversely polarized surface (Love) waves are indicated

193 mogram, i. e. the complete observed frequency band. If we
 194 lower the cutoff frequency to 0.1 Hz (period 10 s), the re-
 195 quired memory drops down to $O(100 \text{ GByte})$. Such calcu-
 196 lations can be done today on PC-clusters that can be in-
 197 expensively assembled and run on an institutional level
 198 (e. g., [8]). In addition, it means that the massive use of
 199 such forward simulations for imaging purposes and phe-
 200 nomenological investigations of wavefield effects is around
 201 the corner. This does not only apply to wave propagation
 202 or imaging on a planetary scale but in the same way to
 203 problems in volcanology, regional seismology, and explo-
 204 ration geophysics.

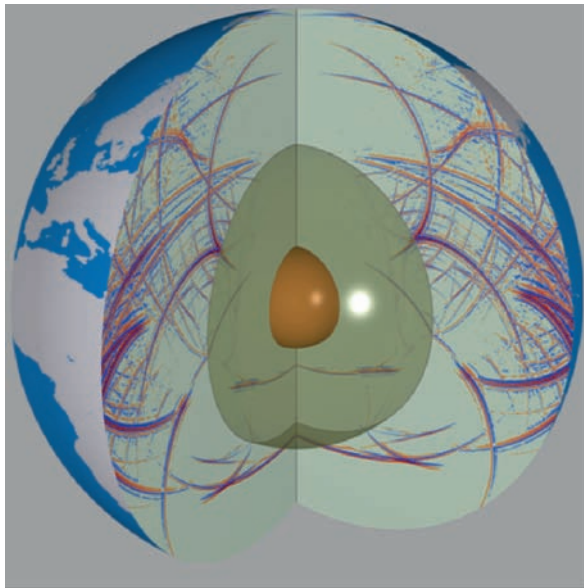
205 An illustration of global wave simulations using the fi-
 206 nite difference method (e. g., [14,54,55,58,109,110,114]) is
 207 shown in Fig. 2 (more details on the methodologies are
 208 given in Sect. “The Evolution of Numerical Methods and
 209 Grids”). The snapshot of the radial component of motion
 210 at a time when the direct P-wave has almost crossed the
 211 Earth reveals the tremendous complexity the wave field
 212 exhibits even in the case of a spherically symmetric Earth
 213 model (PREM, Dziewonski and Anderson 1980 ^{TS2}). The
 214 wavefield with a dominant period of ca. 15 seconds also
 215 highlights the short wavelengths that need to be propa-
 216 gated over very large distances. This is the special require-
 217 ment for computational wave propagation that is quite
 218 different in other fields of computational Earth Sciences.
 219 While the theory of linear elastic wave propagation is well

understood and most numerical methods have been applied
 to it in various forms, the accuracy requirements are so
 high that – particularly when models with complex geo-
 metrical features need to be modeled – there are still open
 questions as to what works best. One of the main goals
 of this paper is to highlight the need to focus on the grid
 generation process for various types of computational grid
 cells (e. g., rectangular, triangular in 2D, and hexahedral
 and tetrahedral in 3D) and the interface to appropriate
 highly accurate solvers for wave propagation problems.

As mentioned above computational modeling of
 strong ground motions following large earthquakes (see
 Fig. 3 for an illustration) is expected to play an increas-
 ingly important role in producing realistic estimates of
 shaking hazard. There are several problems that are cur-
 rently unsolved: (1) to achieve frequencies that are inter-
 esting for earthquake engineers in connection with struc-
 tural damage the near surface velocity structure needs to
 be known and frequencies beyond 5 Hz need to be calcu-
 lated. In most cases this structure is not well known (on
 top of the uncertainties of the lower basin structures) and
 the required frequencies demand extremely large compu-
 tational models. (2) In addition to structural uncertain-
 ties, there are strong dependencies on the particular earth-
 quake rupture process that influence the observed ground
 motions. This suggests that many 3D calculations should
 be carried out for any characteristic earthquake of inter-

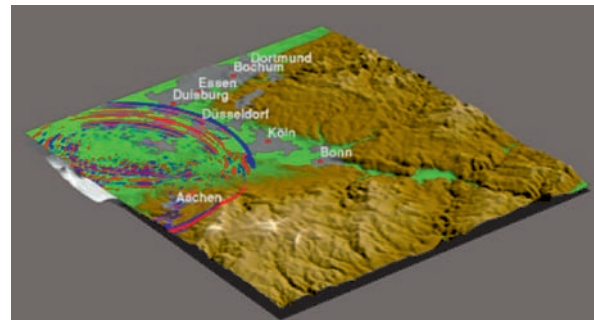
TS2 Do you mean Dziewonski and Anderson 1981?

TS3 Please check. This is not cited in the bibliography.



Simulation of Seismic Wave Propagation in Media with Complex Geometries, Figure 2

Snapshot of wave propagation inside the Earth approx. 25 minutes after an earthquake occurs at the top part of the model. The radial component of motion is shown (blue and red denote positive and negative velocity, resp.). The simulation was carried using an axi-symmetric approximation to the wave equation [55,58] and high-order finite-differences. Motion is allowed in the radial and horizontal directions. This corresponds to the P-SV case in 2D cartesian calculations. Therefore the wavefield contains both P- and S-waves and phase conversions



Simulation of Seismic Wave Propagation in Media with Complex Geometries, Figure 3

Snapshot (horizontal component) for a simulation of the M5.9 Roermond earthquake in the Cologne Basin in 1992 [38]. The 3D sedimentary basin (maximum depth 2 km) leads to strong amplification and prolongation of the shaking duration that correlates well with basin depth. Systematic calculations may help mitigating earthquake induced damage

est, to account for such variations (e. g., Wang et al. 2006, 2007 [153]). (3) The large velocity variations (e. g., 300 m/s up to 8 km/s) require locally varying grid densities which is difficult to achieve with some of the classical numerical methods in use (e. g. finite differences). Some of the potential routes are developed below.

In summary, computational simulation of 3D wave propagation will be more and more a central tool for seismology with application in imaging problems, earthquake rupture problems, questions of shaking hazard, volcano seismology and planetary seismology. In the following we briefly review the history of the application of numerical methods to wave propagation problems and the evolution of computational grids. The increasing complexity of models in terms of geometrical features and range of physical properties imposes the use of novel methodologies that go far beyond the initial approximations based on finite differences.

The Evolution of Numerical Methods and Grids

In this section we give a brief history of the application of numerical methods to the problem of seismic wave propagation. Such a review can not be complete, certainly gives a limited perspective, and only some key references are given. One of the points we would like to highlight is the evolution of the computational grids that are being employed for wave propagation problems and the consequences on the numerical methods of choice now and in the future.

Why do we need numerical approximations to elastic wave propagation problems at all? It is remarkable what we learned about the Earth without them! In the first decades in seismology, modeling of seismic observations was restricted to the calculation of ray-theoretical travel times in spherically symmetric Earth models (e. g., [13,16]). With the advent of computing machines these approaches could be extended to 2D and 3D media leading to ray-theoretical tomography and the images of the Earth's interior that we know today (e. g., [115]). The analytical solution of wave propagation in spherical coordinates naturally leads to spherical harmonics and the possible quasi-analytical solution of wave propagation problems in spherically symmetric media using normal modes. As this methodology leads to complete waveforms the term "waveform inversion" was coined for fitting the waveforms of surface waves by correcting the phase differences for surface waves at particular frequencies (e. g., [118]). This allowed the recovery of seismic velocity models particularly of crust and upper mantle (surface wave tomography). A similar approach in Cartesian

layered geometry led to complete solutions of the wave equation in cylindrical coordinates through the summation of Bessel functions, the reflectivity method [46]. This method was later extended to spherical media through the Earth-flattening transformation [85]. Recently, ray-theory was extended allowing the incorporation of finite-frequency effects (e. g., [84]). The impact on the imaging process is still being debated.

Most of these methods are still today extremely valuable in providing first estimates of 2D or 3D effects and are important for the use in standard seismic processing due to their computational efficiency. Nevertheless, with the tremendous improvements of the quality of seismic observations we strive today to extract much more information on Earth's structure and sources from recorded waveforms. As waveforms are in most places strongly affected by 3D structural variations the application of numerical methods that solve "directly" the partial differential equations descriptive of wave propagation becomes mandatory. This necessity was recognized early on and the developments of numerical wave propagation began in the sixties of the 20th century.

Numerical Methods Applied to Wave Propagation Problems

The **finite-difference** technique was the first numerical method to be intensively applied to the wave propagation problem (e. g., [1,6,61,77,82,83,88,89,116,117]). The partial differentials in the wave equation are replaced by finite differences leading to an extrapolation scheme in time that can either be implicit or explicit. The analysis of such simple numerical schemes led to concepts that are central to basically all numerical solutions of wave propagation problems. First, the discretization in space and time introduces a scale into the problem with the consequence that the numerical scheme becomes dispersive. This numerical dispersion – for the originally non-dispersive problem of purely elastic wave propagation – has the consequence that for long propagation distances wave pulses are no longer stable but disperse. The consequence is, that in any simulation one has to ascertain that enough number of grid points per wavelength are employed so that numerical dispersion is reduced sufficiently. Finding numerical schemes that minimize these effects has been at the heart of any new methodology ever since. Second, the so-called **CFL criterion** [24] that follows from the same theoretical analysis of the numerical scheme basically relates a "grid velocity" – the ratio between the space and time increments dx and dt , respectively – to the largest physical velocity c in the model. In order to have a stable calculation, this ratio has

to be smaller than a constant ε that depends on the specific scheme and the space dimension, a value usually close to unity

$$c \frac{dt}{dx} \leq \varepsilon. \quad (1)$$

This simple relationship has important consequences: When the grid spacing dx must be small, because of model areas with low seismic velocities, then the time step dt has to be made smaller accordingly leading to an overall increase in the number of time steps and thus overall computational requirements. In addition, the early implementations where based on regular rectangular grids, implying that large parts of the model where carrying out unnecessary calculations. As shown below local time-stepping and local accuracy are important ingredients in efficient modern algorithms.

The fairly inaccurate low order spatial finite-difference schemes were later extended to high-order operators [26,48,49,50,51,56,76,103]. Nevertheless, the required number of grid points per wavelength was still large, particularly for long propagation distances. This has led to the introduction of pseudo-spectral schemes, "pseudo" because only the calculations of the derivatives where done in the spectral domain, but the wave equation was still solved in the space-time domain with a time-extrapolation scheme based on finite differences (e. g., Kossloff and Baysal 1982 [10,45,47]). The advantage of the calculation of derivatives in the spectral domain is at hand: The Fourier theorem tells us that by multiplying the spectrum with ik , i being the imaginary unit and k the wavenumber, we obtain an *exact* derivative (exact to numerical precision) on a regular set of grid points. This sounds attractive. However, there are always two sides to the coin. The calculation requires FFTs to be carried out extensively and the original "local" scheme becomes a "global" scheme. This implies that the derivative at a particular point in the computational grid becomes dependent on any other point in the grid. This turns out to be computationally inefficient, in particular on parallel hardware. In addition, the Fourier approximations imply periodicity which makes the implementation of boundary conditions (like the free surface, or absorbing boundary conditions) difficult.

By replacing the basis functions (Fourier series) in the classical **pseudo-spectral method** with Chebyshev polynomials that are defined in a limited domain $(-1,1)$ the problem with the implementation of boundary problems found an elegant solution (e. g., [66,107,108]). However, through the irregular spacing of the Chebyshev collocation points (grid densification at the domain boundaries, see section below) new problems arose with the consequence that this

394 approach was not much further pursued except in com- 445
 395 bination with a multi-domain approach in which the field 446
 396 variables exchange their values at the domain boundaries 447
 397 (e. g., [108]).

398 So far, the numerical solutions described are all based 448
 399 on the *strong* form of the wave equation. The **finite-ele-** 449
 400 **ment method** is another main scheme that found immedi- 450
 401 ate applications to wave propagation problems (e. g., [79]). 451
 402 Finite element schemes are based on solving the *weak* 452
 403 form of the wave equation. This implies that the space- 453
 404 and time-dependent fields are replaced by weighted sums 454
 405 of basis (also called trial) functions defined inside ele- 455
 406 ments. The main advantage of finite element schemes is 456
 407 that elements can have arbitrary shape (e. g., triangles, 457
 408 trapezoidal, hexahedral, tetrahedral, etc.). Depending on 458
 409 the polynomial order chosen inside the elements the spa- 459
 410 tial accuracy can be as desired. The time-extrapolation 460
 411 schemes are usually based on standard finite differences.
 412 There are several reasons why finite-element schemes were
 413 less widely used in the field of wave propagation. First, in
 414 the process a large system matrix needs to be assembled
 415 and must be inverted. Matrix inversion in principle re-
 416 quires global communication and is therefore not optimal
 417 on parallel hardware. Second, in comparison with the fi-
 418 nite-element method, finite- difference schemes are more
 419 easily coded and implemented due their algorithmic sim-
 420 plicity.

421 A tremendous step forward was the introduction of ba- 461
 422 sis functions inside the elements that have spectral accu- 462
 423 racy, e. g., Chebyshev or Legendre polynomials [15,39,65, 463
 424 86,90,98]. The so-called **spectral element scheme** became 464
 425 particularly attractive with the discovery that – by using 465
 426 Legendre polynomials – the matrices that required inver- 466
 427 sion became diagonal [65]. This implies that the scheme 467
 428 does no longer need global communication, it is a lo- 468
 429 cal scheme in which extrapolation to the next time step 469
 430 can be naturally parallelized. With the extension of this 470
 431 scheme to spherical grids using the cubed-sphere dis- 471
 432 cretization [63,64] this scheme is today the method of 472
 433 choice on many scales unless highly complex models need 473
 434 to be initiated.

435 Most numerical schemes for wave propagation prob- 474
 436 lems were based on regular, regular stretched, or hexahe- 475
 437 dral grids. The numerical solution to unstructured grids 476
 438 had much less attention, despite the fact that highly com- 477
 439 plex models with large structural heterogeneities seem to 478
 440 be more readily described with unstructured point clouds. 479
 441 Attempts were made to apply finite volume schemes to this 480
 442 problem [31], and other concepts (like natural neighbor 481
 443 coordinates [7] to find numerical operators that are ap- 482
 444 plicable on unstructured grids [72,73]). These approaches 483
 484
 485
 486
 487
 488
 489
 490
 491
 492
 493

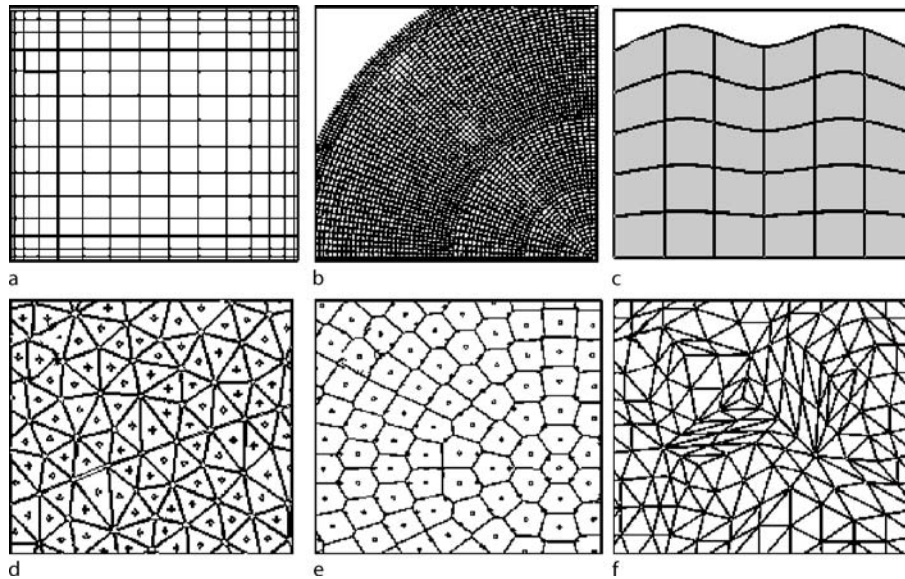
445 were unfortunately not accurate enough to be relevant 446
 447 for 3D problems. Recently, a new flavor of numerical 448
 449 method found application to wave propagation on trian- 449
 450 gular or tetrahedral grids. This combination of a **discon-** 450
 451 **tinuous Galerkin method** with ideas from finite volume 451
 452 schemes [33,70] allows for the first time arbitrary accu- 452
 453 racy in space and time on unstructured grids. While the 453
 454 numerical solution on tetrahedral grids remains computa- 454
 455 tionally slower, there is a tremendous advantage in gener- 455
 456 ating computational grids for complex Earth models. De- 456
 457 tails on this novel scheme are given below. 457

458 Before presenting two schemes (spectral elements and 458
 459 the discontinuous Galerkin method) and some applica- 459
 460 tions in more detail we want to review the evolution of 460
 461 grids used in wave propagation problems.

460 Grids for Wave Propagation Problems

461 The history of grid types used for problems in compu- 461
 462 tational wave propagation is tightly linked to the evolu- 462
 463 tion of numerical algorithms and available computational 463
 464 resources. The latter in the sense that – as motivated in 464
 465 the introduction – even today realistic simulations of wave 465
 466 propagation are still computationally expensive. This im- 466
 467 plies that it is not sufficient to apply stable and simple nu- 467
 468 merical schemes and just use enough grid points per wave- 468
 469 length and/or extremely fine grids for geometrically com- 469
 470 plex models. Optimal mathematical algorithms that mini- 470
 471 mize the computational effort are still sought for as the 471
 472 recent developments show that are outlined in the follow- 472
 473 ing sections. 473

474 In Fig. 4 a number of different computational grids 474
 475 in two space dimensions is illustrated. The simple-most 475
 476 equally-spaced regular finite-difference grid is only of 476
 477 practical use in situations without strong material dis- 477
 478 continuities. With the introduction of the pseudospectral 478
 479 method based on Chebyshev polynomials grids as shown 479
 480 in Fig. 4a grids appeared that are denser near the domain 480
 481 boundaries and coarse in the interior. While this enabled 481
 482 a much more efficient implementation of boundary condi- 482
 483 tions the ratio between the size of the largest to the small- 483
 484 est cell depends on the overall number of grid points per 484
 485 dimension and can be very large. This leads to very small 485
 486 time steps, that can in some way be compensated by grid 486
 487 stretching [9] but overall the problem remains. An ele- 487
 488 gant way of allowing grids to be of more practical shape is 488
 489 by stretching the grids using analytical functions (Fig. 4c, 489
 490 this basically corresponds to a coordinate transformation, 490
 491 e. g., [50,107]). By doing this either smooth surface topog- 491
 492 raphy or smoothly varying internal interfaces can be fol- 492
 493 lowed by the grid allowing a more efficient simulation of 493



Simulation of Seismic Wave Propagation in Media with Complex Geometries, Figure 4

Examples of 2D grids used for wave propagation simulations. **a** Chebyshev grid with grid densification near the domain boundaries. **b** Multidomain finite-difference grid in regular spherical coordinates. **c** Stretched regular finite-difference grid that allows following smoothly varying interface or surface boundaries. **d** Triangular staggered grid following an interface that allows finite-difference type operators. **e** Unstructured grid with associated Voronoi cells for calculations using the finite-volume method. **f** Triangular cells for finite-element type calculations. See text for details and references

494 geometrical features compared to a blocky representation
495 on standard finite difference grids.

496 The problem of global wave propagation using spherical
497 coordinates (here in the two-dimensional, axi-symmet-
498 ric approximation) nicely illustrates the necessity to have
499 spatially varying grid density (e. g., [42,43,53,59,89,109]).
500 The grid shown in Fig. 4b demonstrates that in spheri-
501 cal coordinates a regular discretization leads to grid dis-
502 tances that get smaller and smaller towards the center of
503 the Earth. This is in contrast to what is required to effi-
504 ciently model the Earth's velocity structure: Velocities are
505 small near the surface (requiring high grid density) and in-
506 crease towards the center of the Earth (requiring low grid
507 density). One way of adjusting is by re-gridding the mesh
508 every now and then, in this case doubling the grid spacing
509 appropriately. This is possible, yet it requires interpolation
510 at the domain boundaries that slightly degrades the accu-
511 racy of the scheme.

512 The problems with grid density, and complex surfaces
513 cries for the use of so-called unstructured grids. Let us de-
514 fine an unstructured grid as an initial set of points (a point
515 cloud), each point characterized by its spatial coordinates.
516 We wish to solve our partial differential equations on this
517 point set. It is clear that – with appropriate grid genera-
518 tion software – it is fairly easy to generate such grids that

obey exactly any given geometrical constraints be it in con-
nection with surfaces or velocity models (i. e., varying grid
density). It is important to note that such point clouds can-
not be represented by 2D or 3D matrices as is the case for
regular or regular stretched grid types. This has impor-
tant consequences for the parallelization of numerical
schemes. The first step after defining a point set is to use
concepts from computational geometry to handle the previ-
ously unconnected points. This is done through the idea of
Voronoi cells, that uniquely define triangles and their
neighbors (Delauney triangulation). In Fig. 4d an exam-
ple is shown for a triangular grid that follows an internal in-
terface [72]. For finite-difference type operators on trian-
gular grids a grid-staggering makes sense. Therefore, veloci-
ties would be defined in the center of triangles and stresses at
the triangle vertices. Voronoi cells (Fig. 4e) can be used
as volumetric elements for finite volume schemes [31,73].
For finite-element schemes triangular elements (Fig. 4f,
e. g., [70]) with appropriate triangular shape functions are
quite standard but have not found wide applications in
seismology.

If the grid spacing of a regular finite-difference grid
scheme in 3D would have to be halved this would result
in an overall increase of computation time by a factor of
8 (a factor two per space dimension and another factor 2

519
520
521
522
523
524
525
526
527
528
529
530
531
532
533
534
535
536
537
538
539
540
541
542
543

544 because of the necessary halving of the time step). This
 545 simply means that the accuracy of a specific numerical
 546 scheme and the saving in memory or computation time
 547 is much more relevant in three dimensions. The evolu-
 548 tion of grids in three dimensions is illustrated with ex-
 549 amples in Fig. 5. A geometrical feature that needs to be
 550 modeled correctly particularly in volcanic environments is
 551 the free surface. With standard regular-spaced finite-dif-
 552 ference schemes only a block representation of the surface
 553 is possible (Fig. 5a, e.g., [87,92]). While the specific nu-
 554 merical implementation is stable and converges to correct
 555 solution a tremendous number of grid points is necessary
 556 to achieve high accuracy.

557 Chebyshev grids and regular grids were applied to the
 558 problem of wave propagation in spherical sections (Fig. 5b,
 559 e.g., [52,57]). The advantage of solving the problem in
 560 spherical coordinates is the natural orthogonal coordinate
 561 system that facilitates the implementation of boundary
 562 conditions. However, due to the nature of spherical coordi-
 563 nates the physical domain should be close to the equator
 564 and geographical models have to be rotated accord-
 565 ingly. A highly successful concept for wave propagation in
 566 spherical media was possible through the adoption of the
 567 cubed-sphere approach in combination with spectral-ele-
 568 ments (Fig. 5c, [63,64]). The cubed-sphere discretization
 569 is based on hexahedral grids. Towards the center of the Earth
 570 the grid spacing is altered to keep the number of elements
 571 per wavelength approximately constant.

572 Computational grids for wave propagation based on
 573 tetrahedra (Fig. 5d,e) are only recently being used for
 574 seismic wave propagation in combination with appropri-
 575 ate numerical algorithms such as finite volumes [34] or
 576 discontinuous Galerkin (e.g., [70]). The main advantage
 577 is that the grid generation process is greatly facilitated
 578 when using tetrahedra compared to hexahedra. Generat-
 579 ing point clouds that follow internal velocity structures
 580 and connecting them to tetrahedra are straight forward
 581 and efficient mathematical computations. However, as de-
 582 scribed in more detail below, tetrahedral grids require
 583 more involved computations and are thus less efficient
 584 than hexahedral grids. Complex hexahedral grids – even
 585 for combined modeling of structure and soil (Fig. 5f) are
 586 possible but – at least at present – require a large amount
 587 of manual interaction during the grid generation process.
 588 It is likely that the combination of both grid types (tetra-
 589 hedral in complex regions, hexahedral in less complex re-
 590 gions) will play an important role in future developments.

591 In the following we would like to present two of the
 592 most competitive schemes presently under development,
 593 (1) the spectral element method and (2) the discontinu-
 594 ous Galerkin approach combined with finite-volume flux

595 schemes. The aim is to particularly illustrate the role of the
 596 grid generation process and the pros and cons of the spe-
 597 cific methodologies.

598 3D Wave Propagation on Hexahedral Grids: 599 Soil-Structure Interactions

600 We briefly present the spectral element method (SEM)
 601 based on Legendre polynomials, focusing only on its main
 602 features and on its implementation for the solution of
 603 the elasto-dynamic equations. The SEM can be regarded
 604 as a generalization of the finite element method (FEM)
 605 based on the use of high order piecewise polynomial func-
 606 tions. The crucial aspect of the method is the capability
 607 of providing an arbitrary increase in spatial accuracy sim-
 608 ply enhancing the algebraic degree of these functions (the
 609 spectral degree SD). On practical ground, this operation
 610 is completely transparent to the users, who limit them-
 611 selves to choosing the spectral degree at runtime, leaving
 612 to the computational code the task of building up suit-
 613 able quadrature points for integration and new degrees of
 614 freedom. Obviously, the increasing spectral degree implies
 615 raising the required computational effort.

616 On the other hand, one can also play on the grid refine-
 617 ment to improve the accuracy of the numerical solution,
 618 thus following the standard finite element approach. Spectral
 619 elements are therefore a so-called “ $h - p$ ” method,
 620 where “ h ” refers to the grid size and “ p ” to the degree of
 621 polynomials. Referring to Faccioli et al. [40], Komatitsch
 622 and Vilotte [65], Chaljub et al. [15] for further details, we
 623 briefly remind in the sequel the key features of the spectral
 624 element method adopted. We start from the wave equa-
 625 tion:

$$626 \rho \frac{\partial u^2}{\partial t^2} = \text{div } \sigma_{ij}(u) + f, \quad i, j = 1 \dots d (d = 2, 3) \quad (2)$$

627 where t is the time, $\rho = \rho(x)$ the material density,
 628 $f = f(x, t)$ a known body force distribution and σ_{ij} the
 629 stress tensor. Introducing Hooke’s law:

$$630 \sigma_{ij}(u) = \lambda \text{div } u \delta_{ij} + 2\mu \varepsilon_{ij}(u), \quad (3)$$

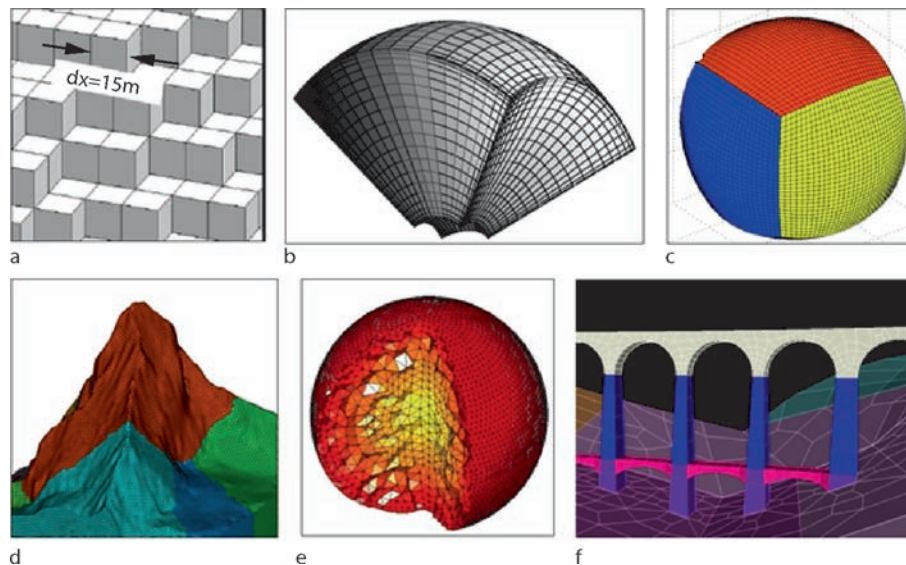
631 where

$$632 \varepsilon_{ij}(u) = \frac{1}{2} \left(\frac{\partial u_i}{\partial x_j} + \frac{\partial u_j}{\partial x_i} \right) \quad (4)$$

633 is the strain tensor, λ and μ are the Lamé coefficients,
 634 and δ_{ij} is the Kronecker symbol, i.e. $\delta_{ij} = 1$ if $i = j$ and
 635 $\delta_{ij} = 0$, otherwise.

636 As in the FEM approach, the dynamic equilibrium
 637 problem for the medium can be stated in the weak, or vari-
 638 ational form, through the principle of virtual work [121]

TS4 Please add references.



Simulation of Seismic Wave Propagation in Media with Complex Geometries, Figure 5

Examples of 3D grids. **a** Stair-step representation of a complex free surface with finite-difference cells. **b** Chebyshev grid in spherical coordinates for a spherical section. **c** Cubed sphere grid used for spectral-element and multi-domain Chebyshev calculations. **d** Tetrahedral grid of the Matterhorn. **e** Tetrahedral grid of the Earth's interior with the grid density tied to the velocity model. **f** Hexahedral grid of bridge structure and subsurface structure for spectral-element calculations. See text for details and references [TS4](#)

639 and through a suitable discretization procedure that de- 640
 640 pends on the numerical approach adopted, can be written 641
 641 as an ordinary differential equations system with respect 642
 642 to time:

$$643 \quad [M] \ddot{\mathbf{U}}(t) + [K] \mathbf{U}(t) = \mathbf{F}(t) + \mathbf{T}(t) \quad (5)$$

644 where matrices $[M]$ and $[K]$, respectively the mass and 645
 645 the stiffness matrix, vectors \mathbf{F} and \mathbf{T} are due to the con- 646
 646 tributions of external forces and traction conditions, re- 647
 647 spectively. In our SE approach, \mathbf{U} denotes the displace- 648
 648 ment vector at the Legendre–Gauss–Lobatto (LGL) nodes, 649
 649 that correspond to the zeroes of the first derivatives of Leg- 650
 650 endre polynomial of degree N . The advancement of num- 651
 651 erical solution in time is provided by the explicit 2nd order 652
 652 leap-frog scheme. This scheme is conditionally stable 653
 653 and must satisfy the well known and already mentioned 654
 654 Courant–Friedrichs–Levy (CFL) condition. The key fea- 655
 655 tures of the SE discretization are described in the follow- 656
 656 ing.

657 Like in the FEM standard technique, the computa- 658
 658 tional domain may be split into quadrilaterals in 2D or 659
 659 hexahedral in 3D, both the local distribution of grid points 660
 660 within the single element and the global mesh of all the 661
 661 grid points in the domain must be assigned. Many of these 662
 662 grid points are shared amongst several spectral elements. 663
 663 Each spectral element is obtained by a mapping of a master

664 element through a suitable transformation and all compu- 665
 665 tations are performed on the master element. Research is 666
 666 in progress regarding the introduction of triangular spec- 667
 667 tral elements [80]. The nodes within the element where 668
 668 displacements and spatial derivatives are computed, on 669
 669 which volume integrals are evaluated, are not necessar- 670
 670 ily equally spaced (similar to the Chebyshev approach in 671
 671 pseudospectral methods mentioned above). The interpola- 672
 672 tion of the solution within the element is done by Lag- 673
 673 range polynomials of suitable degree. The integration in 674
 674 space is done through Legendre–Gauss–Lobatto quadra- 675
 675 ture formula.

676 Thanks to this numerical strategy, the exponential ac- 677
 677 curacy of the method is ensured and the computational 678
 678 effort minimized, since the mass matrix results to be di- 679
 679 agonal. The spectral element (SE) approach developed by 680
 680 Faccioli et al. [40] has been recently implemented in the 681
 681 computational code GeoELSE (GeoElasticity by Spectral 682
 682 Elements [93,102,120] for 2D/3D wave propagation an- 683
 683 alyzes. The most recent version of the code includes: (i) 684
 684 the capability of dealing with fully unstructured compu- 685
 685 tational domains, (ii) the parallel architecture, and (iii) 686
 686 visco-plastic constitutive behavior [30]. The mesh can be 687
 687 created through an external software (e.g., CUBIT [25]) 688
 688 and the mesh partitioning is handled by METIS [81] [TS5](#).

[TS5](#) I changed the wording. Please check.

Hexahedral Grids

As already mentioned in the SEM here presented the computational domain is decomposed into a family of non overlapping quadrilaterals in 2D or hexahedra in 3D. The grid discretization should be suitable to accurately propagate up to certain frequencies. Obviously, owing to the strong difference of the mechanical properties between soft-soil and rock-soil (or building construction material) and to the different geometrical details as well, the grid refinement needed in the various parts of the model varies substantially. Therefore, a highly unstructured mesh is needed to minimize the number of elements. While 3D unstructured tetrahedral meshes can be achieved quite easily with commercial or non commercial software, the creation of a 3D non structured hexahedral mesh is still recognized as a challenging problem. In the following paragraph we provide state of the art results concerning the mesh creation.

Grid Generation

Hexahedral grids have more severe restrictions in meshing efficiently. This is basically related to the intrinsic difficulty that arises from the mapping of the computational domain with this particular element. As a consequence automatic procedures have difficulty capturing specific boundaries, create poor quality elements, the assigned size is difficult to be preserved and the generation process is usually much slower compared to the tetrahedral mesh generation algorithms. On the other hand the advantages of hexahedral meshes are usually related to the lower computational cost of the wave propagation solutions with respect to the one based on triangular meshes or hexahedral structured grids (like in the finite difference method).

Nevertheless certain problems can be addressed reasonably well with specific solutions. A quite typical case in earthquake seismology is the study of the alluvial basin response under seismic excitation. In handling this problem, a first strategy is to try to “honor” the interface between the sediment (soft soil) and the bedrock (stiff soil). The two materials are divided by a physical interface and the jump in the mechanical properties is strictly preserved. The major drawback of this approach is that usually it requires strong skills from the user to build-up the mesh and a significant amount of working time (Fig. 6). Given that the “honoring approach” is not always feasible in a reasonable time (or with a reasonable effort) a second strategy is worth to be mentioned: The so called “not honoring” procedure. In this second case the mesh is refined in proximity of the area where the soft deposit are localized but the elements do not respect the interface. On a practical ground

the mechanical properties are assigned node by node and the sharp jump is smoothed through the Lagrange interpolation polynomial and substituted with smeared interfaces (Fig. 7). At the present time it is still strongly under debate if it is worth to honor or not the physical interfaces.

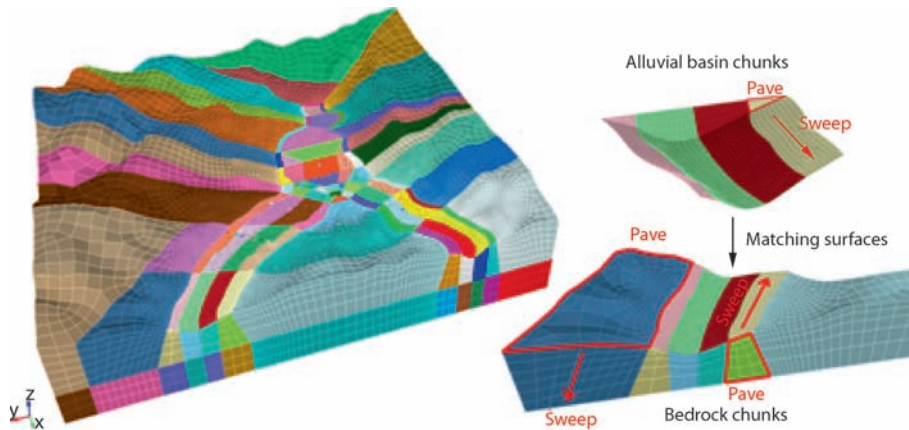
Finally, we highlight the fact that meshing software (e.g., CUBIT [25]) is available that seems to be extremely promising and potentially very powerful for the creation of geophysical and seismic engineering unstructured hexahedral meshes. Further very interesting mesh generation procedures based on hexahedral are under investigation [99].

Scale Problem with Structure and Soil

In engineering practice one of the most common approaches to design buildings under seismic load is the imposition of an acceleration time history to the structure, basically acting like an external load. An excellent example of this technique can be found in recent publications (e.g., [68,69]) and in the study of the so-called “urban-seismology”, recently presented by Fernandez-Ares et al. (2006) [93]. In this case the goal is to understand how the presence of an entire city can modify the incident wavefield. Due to the size of the simulation and the number of buildings, the latter are modeled as single degrees of freedom oscillators. The interaction between soil and structure is preserved but the buildings are simplified. For important structure (e.g.: Historical buildings, world heritage buildings, hospitals, schools, theaters, railway and highways) it is worth to provide an ad-hoc analysis capable to take into account the full complexity of the phenomena.

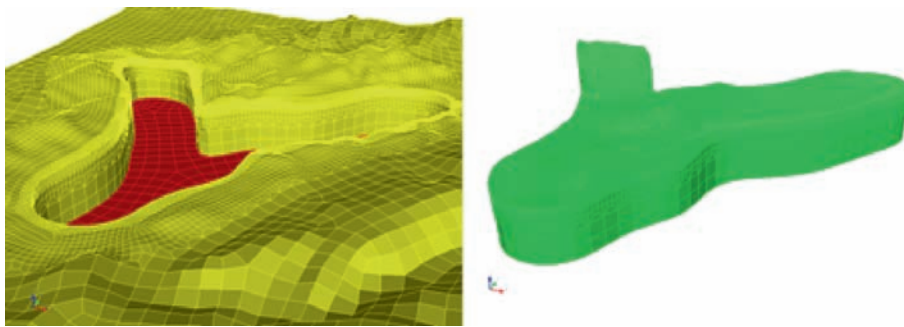
Here we present an example of a fully coupled modeling (Fig. 8): A railway bridge and its geological-topographical surroundings. The Acquasanta bridge on the Genoa-Ovada railway, North Italy, is located in the Genoa district and represents a typical structure the ancestor of which can be traced back to the Roman “Pont du Gard”. This structural type did not change significantly along the centuries, thanks to the excellent design achieved no less than 1900 years ago. The Acquasanta bridge structure is remarkable both for the site features and the local geological and geomorphological conditions. The foundations of several of the piers rest on weak rock; moreover, some instability problems have been detected in the past on the valley slope towards Ovada.

Several simulations have been performed with GeoELSE, in order to evaluate the influence of seismic site effects on the dynamic response of the Acquasanta bridge. A fully coupled 3D soil-structure model was designed: The grid is characterized by a “subvertical fault”



Simulation of Seismic Wave Propagation in Media with Complex Geometries, Figure 6

3D numerical model used for the simulations of ESG06 “Grenoble Benchmark”. “Honoring” technique: The computational domain is subdivided into small chunks and each one is meshed starting from the alluvial basin down to the bedrock. For simplicity only the spectral elements are shown without LGL nodes



Simulation of Seismic Wave Propagation in Media with Complex Geometries, Figure 7

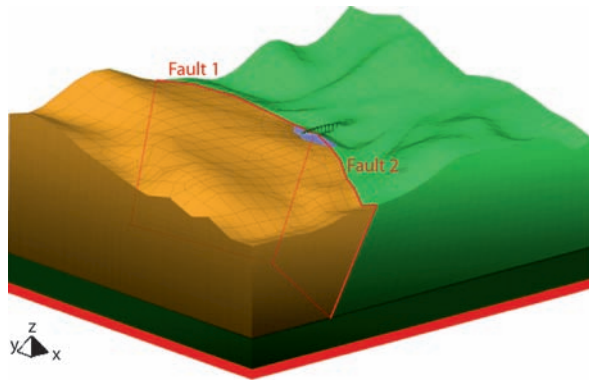
3D numerical model used for the simulations of ESG06 “Grenoble Benchmark”. “Not Honoring” technique: The computational domain is meshed with a coarse mesh and then refined twice approximately in the area where the alluvial basin is located

787 between calcareous schists and serpentine rocks. This is in
 788 accordance with available data, even if further investiga-
 789 tions in future should identify more in detail the tectonic
 790 structure of the area. The geometry of weathered materials
 791 overlaying the calcareous schists on the Ovada side has
 792 been assumed according to available information. The di-
 793 mension of hexahedral elements ranges some tens of cen-
 794 timeters to about 1000 m. With such a model, the problem
 795 can be handled in its 3D complexity and we can exam-
 796 ine the following aspects that are usually analyzed under
 797 restrictive and simplified assumptions: (i) soil-structure
 798 interaction, (ii) topographic amplification, (iii) soft soil
 799 amplification (caused by the superficial alluvium deposit
 800 shown in cyan), (iv) subvertical fault (red line) between
 801 the schists, on the Ovada side, and serpentine rock, on the
 802 Genoa side. For excitation a shear plane wave (x -direction)
 803 was used (Ricker wavelet, $f_{max} = 3$ Hz, $t_0 = 1.0$ s. and

amplitude = 1 mm) propagating vertically from the bot- 804
 tom (red elements in Fig. 8). 805

In Fig. 9 we present some snapshots of the modulus 806
 of the displacement vector and the magnified deformed 807
 shape of the bridge. It is worth to note that at $T = 2$ s the 808
 motion of the bridge is almost in-plane (direction x), while 809
 at $T = 4$ s is clearly evident how the coupling between the 810
 in-plane and out-plane (y -direction) motion starts to be 811
 important. 812

The study of the soil-structure interaction problem 813
 could be easily enhanced (i) improving the input excita- 814
 tion of the model here presented and (ii) taking into ac- 815
 count complex constitutive behavior both from the soil 816
 and the structure side. The former is already available in 817
 GeoELSE thanks to the recent implementation [41,93] of 818
 the domain reduction method (DRM), a methodology that 819
 divides the original problem into two simpler ones [4,119], 820



Simulation of Seismic Wave Propagation in Media with Complex Geometries, Figure 8

3D model of Acquasanta bridge and the surrounding geological configuration. The investigated area is 2 km in length, 1.75 km in width and 0.86 km in depth. The model was designed to propagate waves up to 5 Hz with a $SD = 3$ (Order 4) and has 38,569 hexahedral elements and 1,075,276 grid points. The contact between calcareous schists (brown color) and serpentine rocks (green color) is modeled with two sub-vertical faults (red-line). Cyan color represents the alluvial and weathered deposits

to overcome the problem of multiple physical scales that is created by a seismic source usually located at some depth on rock far away from the structure with typical element size of the order of meters and located over a relatively small area (less than 1 km^2) on soft deposit. The latter still need to be improved because of the lack of a complete tool capable to handle in 3D non linear soil behavior, non-linear structural behavior and the presence of the water, that play a crucial role in the failure of buildings. Partial response to this problem can be found in the recent work of Bonilla et al. [5] and in the visco-plastic rheology recently introduced in GeoELSE (di Prisco, 2006 [TS3]).

3D Wave Propagation on Tetrahedral Grids: Application to Volcanology

As indicated above, the simulation of a complete, highly accurate wave field in realistic media with complex geometry is still a great challenge. Therefore, in the last years a new, highly flexible and powerful simulation method has been developed that combines the Discontinuous Galerkin (DG) Method with a time integration method using Arbitrary high order DERivatives (ADER) of the approximation polynomials. The unique property of this numerical scheme is, that it achieves arbitrarily high approximation order for the solution of the governing seismic wave equation in space and time on structured and unstructured meshes in two and three space dimensions.

Originally, this new ADER-DG approach [32,35] was introduced for general linear hyperbolic equation systems with constant coefficients or for linear systems with variable coefficients in conservative form. Then, the extension to non-conservative systems with variable coefficients and source terms and its particular application to the simulation of seismic waves on unstructured triangular meshes in two space dimensions was presented [70]. And finally, the further extension of this approach to three-dimensional tetrahedral meshes has been achieved [33]. Furthermore, the accurate treatment of viscoelastic attenuation, anisotropy and poroelasticity has been included to handle more complex rheologies [28,29,71]. The governing system of the three-dimensional seismic wave equations is hereby formulated in velocity-stress and leads to the hyperbolic system of the form

$$\frac{\partial \mathbf{Q}_p}{\partial t} + A_{pq} \frac{\partial \mathbf{Q}_q}{\partial \xi} + B_{pq} \frac{\partial \mathbf{Q}_q}{\partial \eta} + C_{pq} \frac{\partial \mathbf{Q}_q}{\partial \zeta} = S_p, \quad (6)$$

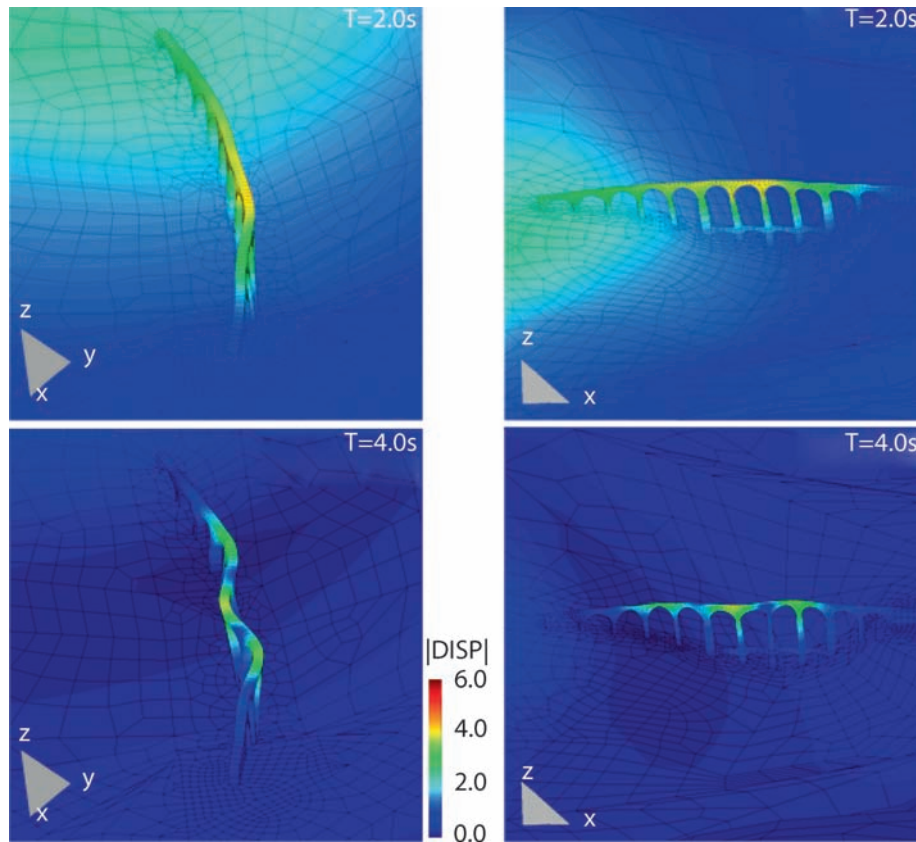
where the vector \mathbf{Q} of unknowns contains the six stress and the three velocity components and S is the source term. The Jacobian matrices A , B and C include the material values as explained in detail in [33,70].

The ADER-DG Method: Basic Concepts

The ADER-DG method is based on the combination of the ADER time integration approach [113], originally developed in the finite volume (FV) framework [96,97,111] and the Discontinuous Galerkin finite element method [18,19,20,21,22,23,91]. As described in detail in [33] in the ADER-DG approach the solution is approximated inside each tetrahedron by a linear combination of space-dependent polynomial basis functions and time-dependent degrees of freedom as expressed through

$$(\mathbf{Q}_h)_p(\xi, \eta, \zeta, t) = \hat{\mathbf{Q}}_{pl}(t) \Phi_l(\xi, \eta, \zeta), \quad (7)$$

where the basis functions Φ_l form an orthogonal basis and are defined on the canonical reference tetrahedron. The unknown solution inside each element is then approximated by a polynomial, whose coefficients – the degrees of freedom Q_{pl} – are advanced in time. Hereby, the solution can be discontinuous across the element interfaces, which allows the incorporation of the well-established ideas of numerical flux functions from the finite volume framework [75,112]. To define a suitable flux over the element surfaces, so-called Generalized Riemann Problems (GRP) are solved at the element interfaces. The GRP solution provides simultaneously a numerical flux function as well as a time-integration method. The main idea is a Taylor



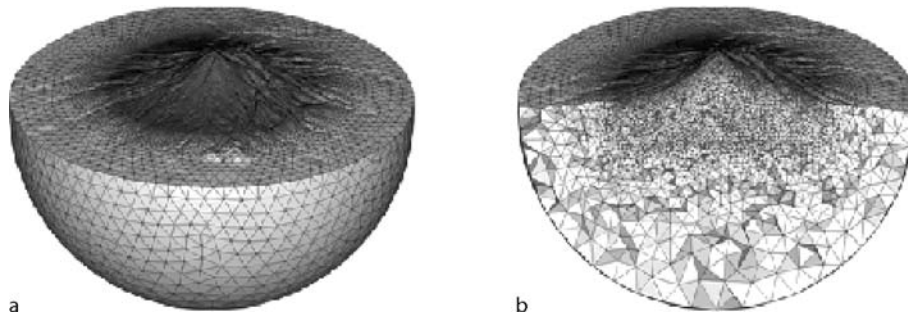
Simulation of Seismic Wave Propagation in Media with Complex Geometries, Figure 9
 Snapshots of the modulus of the displacement vector and the magnified deformed shape of the bridge (in mm)

892 expansion in time in which all time derivatives are re-
 893 placed by space derivatives using the so-called Cauchy-
 894 Kovalevski procedure which makes recursive use of the
 895 governing differential Eq. (6). The numerical solution of
 896 Eq. (6) can thus be advanced by one time step without in-
 897 termediate stages as typical e. g. for classical Runge-Kutta
 898 time stepping schemes. Due to the ADER time integra-
 899 tion technique the same approximation order in space and
 900 time is achieved automatically. Furthermore, the projec-
 901 tion of the elements in physical space onto a canonical refer-
 902 ence element allows for an efficient implementation, as
 903 many computations of three-dimensional integrals can be
 904 carried out analytically beforehand. Based on a numerical
 905 convergence analysis this new scheme provides arbitrary
 906 high order accuracy on unstructured meshes. Moreover,
 907 due to the choice of the basis functions in Eq. (7) for the
 908 piecewise polynomial approximation [23], the ADER-DG
 909 method shows even spectral convergence.

Grid Generation: Unstructured Triangulations and Tetrahedralization

910 Both tetrahedral and hexahedral elements are effectively
 911 used to discretize three-dimensional computational do-
 912 mains and model wave propagation with finite element
 913 type methods. Tetrahedrons can be the right choice be-
 914 cause of the robustness when meshing any general shape.
 915 Hexahedrons can be the element of choice due to their
 916 ability to provide more efficiency and accuracy in the com-
 917 putational process. Furthermore, techniques for automatic
 918 mesh generation, gradual mesh refinement and coarsening
 919 are generally much more robust for tetrahedral meshes in
 920 comparison to hexahedral meshes. Straightforward tetra-
 921 hedral refinement schemes, based on longest-edge divi-
 922 sion, as well as the extension to adaptive refinement or
 923 coarsening procedures of a refined mesh exist [3,12]. In
 924 addition, parallel strategies for refinement and coarsening
 925 of tetrahedral meshes have been developed [27].
 926

927 Less attention has been given to the modification
 928 of hexahedral meshes. Methods using iterative octrees
 929



Simulation of Seismic Wave Propagation in Media with Complex Geometries, Figure 10

Tetrahedral mesh for the model of the volcano Merapi. The zone of interest, such as the free surface topography and the volcano's interior are discretized by a fine mesh, whereas the spatial mesh is gradually coarsened towards the model boundaries

930 have been proposed [74,95], but these methods often
 931 result in nonconformal elements that cannot be accom-
 932 modated by some solvers. Lately also conformal refine-
 933 ment and coarsening strategies for hexahedral meshes
 934 have been proposed [2]. Other techniques insert non-hex-
 935 ahedral elements that result in hybrid meshes that need
 936 special solvers that can handle different mesh topologies.
 937 Commonly, the geometrical problems in geosciences arise
 938 through rough surface topography, as shown for the Mer-
 939 api volcano in Fig. 10, and internal material boundaries
 940 of complex shape that lead to wedges, and overturned or
 941 discontinuous surfaces due to folding and faulting. How-
 942 ever, once the geometry of the problem is defined by the
 943 help of modern computer aided design (CAD) software,
 944 the meshing process using tetrahedral elements is autom-
 945 atic and stable. After the mesh generation process, the
 946 mesh vertices, the connectivity matrix and particular in-
 947 formation about boundary surfaces are typically imported
 948 to a solver.

949 The computational possibilities and algorithmic flexi-
 950 bility of a particular solver using the ADER-DG approach
 951 for tetrahedral meshes are presented in the following.

952 Local Accuracy: p -Adaptation

953 In many large scale applications the computational do-
 954 main is much larger than the particular zone of interest.
 955 Often such an enlarged domain is chosen to avoid effects
 956 from the boundaries that can pollute the seismic wave field
 957 with possible, spurious reflections. Therefore, a greater
 958 number of elements has to be used to discretize the do-
 959 main describing the entire model. However, in most cases
 960 the high order accuracy is only required in a restricted area
 961 of the computational domain and it is desirable to choose
 962 the accuracy that locally varies in space. This means, that it
 963 must be possible to vary the degree p of the approximation

964 polynomials locally from one element to the other [36]. As
 965 the ADER-DG method uses a hierarchical order of the ba-
 966 sis functions to construct the approximation polynomials,
 967 the corresponding polynomial coefficients, i. e. the degrees
 968 of freedom, for a lower order polynomial are always a sub-
 969 set of those of a higher-order one. Therefore, the computa-
 970 tion of fluxes between elements of different approximation
 971 orders can be carried out by using only the necessary part
 972 of the flux matrices.

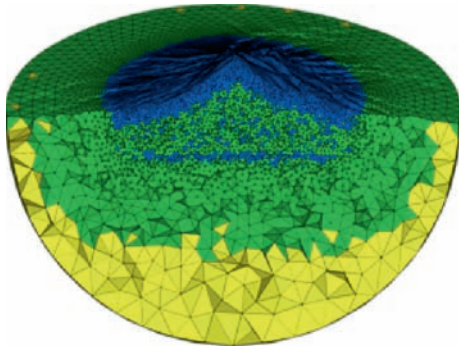
973 Furthermore, the direct coupling of the time and space
 974 accuracy via the ADER approach automatically leads to
 975 a local adaptation also in time accuracy, which often is re-
 976 ferred to as p -adaptivity. In general, the distribution of the
 977 degree p might be connected to the mesh size h , i. e. the
 978 radius of the inscribed sphere of a tetrahedral element. In
 979 particular, the local degree p can be coupled to the mesh
 980 size h via the relations

$$981 \quad p = p_{\min} + (p_{\max} - p_{\min}) \left(\frac{h - h_{\min}}{h_{\max} - h_{\min}} \right)^r, \quad (8)$$

$$982 \quad p = p_{\max} - (p_{\max} - p_{\min}) \left(\frac{h - h_{\min}}{h_{\max} - h_{\min}} \right)^r, \quad (9)$$

983 where the choice of the power r determines the shape of
 984 the p -distribution. Note, that depending on the choice of
 985 the first term and the sign the degree p can increase as in
 986 Eq. (8) or decrease as in Eq. (9) with increasing h , starting
 987 from a minimum degree p_{\min} up to a maximum degree
 988 p_{\max} . This provides additional flexibility for the distribu-
 989 tion of p inside the computational domain. An example of
 990 a p -distribution for the volcano Merapi is given in Fig. 11.

991 Here the idea is to resolve the slowly propagating sur-
 992 face waves with high accuracy, whereas the waves propa-
 993 gating towards the absorbing model boundaries pass
 994 through a zone of low spatial resolution. This approach
 995 leads to numerical damping due to an amplitude decay
 996 that reduces possible boundary reflections. Furthermore,



Simulation of Seismic Wave Propagation in Media with Complex Geometries, Figure 11

The local degree p of the approximation polynomial depends on the insphere radius of each tetrahedral element and is given in color code. Close to the surface topography an approximation polynomial of degree $p = 5$ (blue) is used, whereas in depth the degree is reduced to $p = 4$ (green) and $p = 3$ (yellow)

997 the computational cost is reduced significantly due to the
998 strongly reduced number of total degrees of freedom in the
999 model.

1000 Local Time Stepping: Δt -Adaptation

1001 Geometrically complex computational domains or spatial
1002 resolution requirements often lead to meshes with small
1003 or even degenerate elements. Therefore, the time step for
1004 explicit numerical schemes is restricted by the ratio of the
1005 size h of the smallest element and the corresponding maxi-
1006 mum wave speed in this element. For global time stepping
1007 schemes all elements are updated with this extremely re-
1008 strictive time step length leading to a large amount of it-
1009 erations. With the ADER-DG approach, time accurate lo-
1010 cal time stepping can be used, such that each element is
1011 updated by its own, optimal time step [36]. Local time-
1012 stepping was used in combination with the finite-differ-
1013 ence method by Falk et al. (1996) [TS6] and Tessmer [106].

1014 An element can be updated to the next time level if its
1015 actual time level and its local time step Δt fulfill the follow-
1016 ing condition with respect to all neighboring tetrahedra n :

$$1017 \quad t + \Delta t \leq \min(t_n + \Delta t_n). \quad (10)$$

1018 Figure 12 is visualizing the evolution of four elements (I,
1019 II, III and IV) in time using the suggested local time step-
1020 ping scheme. A loop cycles over all elements and checks
1021 for each element, if condition (10) is fulfilled. At the ini-
1022 tial state all elements are at the same time level, however,
1023 element II and IV fulfill condition (10) and therefore can
1024 be updated. In the next cycle, these elements are already
1025 advanced in time (grey shaded) in cycle 1. Now elements

I and IV fulfill condition (10) and can be updated to their
1026 next local time level in cycle 2. This procedure continues
1027 and it is obvious, that the small element IV has to be up-
1028 dated more frequently than the others. A synchronization
1029 to a common global time level is only necessary, when data
1030 output at a particular time level is required as shown in
1031 Fig. 12.
1032

Information exchange between elements across inter-
1033 faces appears when numerical fluxes are calculated. These
1034 fluxes depend on the length of the local time interval over
1035 which a flux is integrated and the corresponding element is
1036 evolved in time. Therefore, when the update criterion (10)
1037 is fulfilled for an element, the flux between the element it-
1038 self and its neighbor n has to be computed over the local
1039 time interval:
1040

$$1041 \quad \tau_n = [\max(t, t_n), \min(t + \Delta t, t_n + \Delta t_n)]. \quad (11)$$

As example, the element III fulfills the update crite-
1042 rion (10) in cycle 5 (see Fig. 12). Therefore, when com-
1043 puting the fluxes only the remaining part of the flux given
1044 by the intervals in Eq. (11) has to be calculated. The other
1045 flux contribution was already computed by the neighbors
1046 II and IV during their previous local updates. These flux
1047 contributions have been accumulated and were stored into
1048 a memory variable and therefore just have to be added.
1049

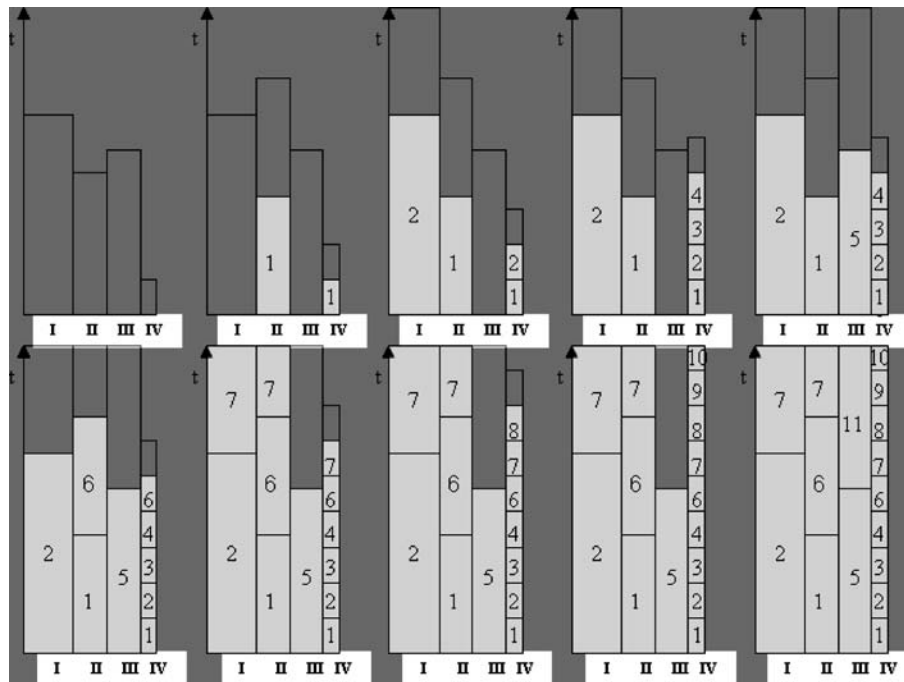
Note that e. g. element IV reaches the output time af-
1050 ter 10 cycles and 9 local updates, which for a global time
1051 stepping scheme would require $9 \times 4 = 36$ updates for the
1052 all four elements. With the proposed local time stepping
1053 scheme only 16 updates are necessary to reach the same
1054 output time with all elements as indicated by the final
1055 number of grey shaded space time elements in Fig. 12.
1056

Comparing these numbers leads to a speedup fac-
1057 tor of 2.25. For strongly heterogeneous models and local
1058 time step lengths this factor can become even more pro-
1059 nounced. However, due to the asynchronous update of el-
1060 ements that might be spatially very close to each other the
1061 mesh partitioning for parallel computations becomes an
1062 important and difficult issue. Achieving a satisfying load
1063 balancing is a non-trivial task and still poses some unre-
1064 solved problems as explained in the following.
1065

1066 Mesh Partitioning and Load Balancing

1067 For large scale applications it is essential to design a par-
1068 allel code that can be run on massively parallel super-
1069 computing facilities. Therefore, the load balancing is an
1070 important issue to use the available computational re-
1071 sources efficiently. For global time stepping schemes with-
1072 out p -adaptation standard mesh partitioning as done e. g.

TS6 Please check. Which reference do you mean exactly?



Simulation of Seismic Wave Propagation in Media with Complex Geometries, Figure 12

Visualization of the local time stepping scheme. The actual local time level t is at the top of the gray shaded area with numbers indicating the cycle, in which the update was done. Dotted lines indicate the local time step length Δt with which an element is updated

1073 by METIS [60] is sufficient to get satisfying load balanc- 1096
 1074 ing. The unstructured tetrahedral mesh is partitioned into 1097
 1075 subdomains that contain an equal or at least very similar 1098
 1076 number of elements as shown in Fig. 13. Therefore, each 1099
 1077 processor has to carry out a similar amount of calcula- 1100
 1078 tions. However, if p -adaptation is applied, the partition- 1101
 1079 ing is more sophisticated as one subdomain might have 1102
 1080 many elements of high order polynomials whereas another 1103
 1081 might have the same number of elements but with lower 1104
 1082 order polynomials. Therefore, the parallel efficiency is re- 1105
 1083 stricted by the processor with the highest work load. How- 1106
 1084 ever, this problem can usually be solved by weighted par- 1107
 1085 titioning algorithms, e. g. METIS. 1108

1086 In the case of local time stepping, mesh partitioning 1109
 1087 becoming a much more difficult task. One solution is to 1110
 1088 divide the computational domain into a number of zones, 1111
 1089 that usually contain a geometrical body or a geological 1112
 1090 zone that typically is meshed individually with a particular 1113
 1091 mesh spacing h and contains a dominant polynomial order. 1114
 1092 Then each of these zones is partitioned separately into 1115
 1093 subdomains of approximately equal numbers of elements. 1116
 1094 Then each processor receives a subdomain of each zone, 1117
 1095 which requires a similar amount of computational work 1118

1096 as shown in Fig. 13. In particular, the equal distribution of 1097
 1098 tetrahedrons with different sizes is essential in combina- 1099
 1100 tion with the local time stepping technique. Only if each 1101
 1102 processor receives subdomains with in total give a similar 1103
 1104 amount of small and large elements, the work load is 1104
 1105 balanced. The large elements have to be updated less fre- 1105
 1106 quently than the smaller elements and therefore are com- 1106
 1107 putationally cheaper. Note, that the separately partitioned 1107
 1108 and afterwards merged zones lead to non-connected sub- 1108
 1109 domains for each processor (see Fig. 13). This increases 1109
 1110 the number of element surfaces between subdomains of 1110
 1111 different processors and therefore increases the communica- 1111
 1112 tion required. However, communication is typically low 1112
 1113 as the degrees of freedom have to be exchanged only once 1113
 1114 per time step and only for tetrahedrons that have an inter- 1114
 1115 face at the boundary between subdomains. Therefore, the 1115
 1116 improvements due to the new load balancing approach are 1116
 1117 dominant and outweigh the increase in communication. 1117
 1118

1114 However, care has to be taken as the distribution of 1114
 1115 the polynomial degree p or the seismic velocity structure 1115
 1116 might influence the efficiency of this grouped partitioning 1116
 1117 technique. A profound and thorough mesh partitioning 1117
 1118 method is still a pending task as the combination of lo- 1118

cal time stepping and p -adaptivity requires a new weighting strategy of the computational cost for each tetrahedral element considering also the asynchronous element update. The automatic partitioning of unstructured meshes with such heterogeneous properties together with the constraint of keeping the subdomains as compact as possible to avoid further increase of communication is still subject to future work.

In Fig. 13 an example of a grouped partition of the tetrahedral mesh is shown for 4 processors. Two non-connected subdomains indicated by the same color are assigned to each processor including small – and therefore computationally expensive – tetrahedrons that are updated frequently due to their small time step, and much larger elements that typically are cheap due to their large time step. This way, the work load often is balanced sufficiently well over the different processors.

Relevance of High Performance Computing: Application to Merapi Volcano

In recent years the development of the ADER-DG algorithm including the high order numerical approximation in space and time, the mesh generation, mesh adaptation, parameterization, and data visualization form the basis of an efficient and highly accurate seismic simulation tool. Realistic large scale applications and their specific requirements will further guide these developments. On the other hand, the study and incorporation of geophysical processes that govern seismic wave propagation insures, that the simulation technology matches the needs and addresses latest challenges in modern computational seismology. Hereby, the accurate modeling of different source mechanisms as well as the correct treatment of realistic material properties like anelasticity, viscoplasticity, porosity and highly heterogeneous, scattering media will play an important role.

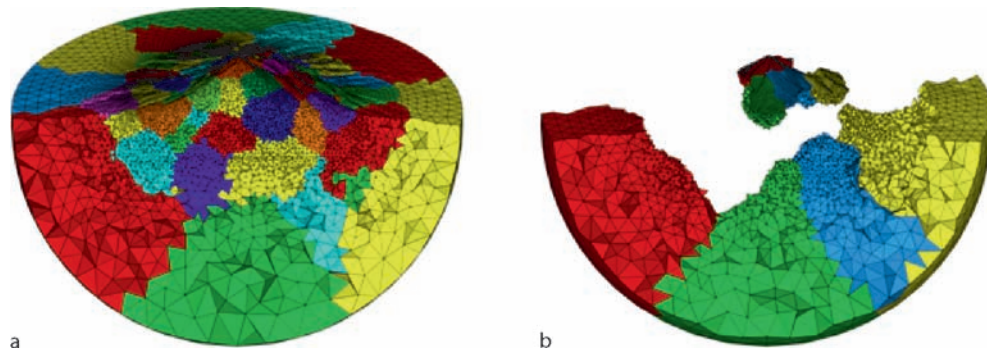
However, only the combination of this state-of-the-art simulation technology with the most powerful supercomputing facilities actually available can provide excellent conditions to achieve scientific progress for realistic, large scale applications. This combination of modern technologies will substantially contribute to resolve current problems, not only in numerical seismology, but will also influence other disciplines. The phenomenon of acoustic, elastic or seismic wave propagation is encountered in many different fields. Beginning with the classical geophysical sciences seismology, oceanography, and volcanology such waves also appear in environmental geophysics, atmospheric physics, fluid dynamics, exploration geophysics, aerospace engineering or even medicine.

With the rapid development of modern computer technology and the development of new highly accurate simulation algorithms computer modeling just started to herald a new era in many applied sciences. The 3D wave propagation simulations in realistic media require a substantial amount of computation time even on large parallel computers. Extremely powerful national supercomputers already allow us to run simulations with unrivaled accuracy and resolution. However, using the extremely high accuracy and flexibility of new simulation methods on such massively parallel machines the professional support of experts in supercomputing is absolutely essential. Only professional porting, specific CPU-time and storage optimizations of current software with respect to continuously changing compilers, operating systems, hardware architectures or simply personnel, will ensure the lifetime of new simulation technologies accompanied by ongoing improvements and further developments. Additionally, the expertise and support in the visualization of scientific results using technologies of Virtual Reality for full 3D models not only enhances the value of simulations results but will support data interpretation and awake great interest in the new technology within a wide research community.

As an example, volcano monitoring plays an increasingly important role in hazard estimation in many densely populated areas in the world. Highly accurate computer modeling today is a key issue to understand the processes and driving forces that can lead to dome building, eruptions or pyroclastic flows. However, data of seismic observations at volcanoes are often very difficult to interpret. Inverting for the source mechanism, i. e. seismic moment tensor inversion, or just locating an exact source position is often impossible due to the strongly scattered wave field due to an extremely heterogeneous material distribution inside the volcano. Furthermore, the rough topography alone can affect the wave field by its strongly scattering properties as shown in Fig. 14.

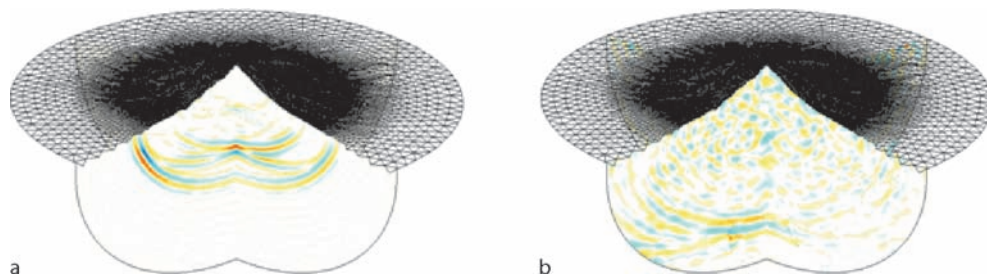
Therefore, it is fundamental to understand the effects of topography and scattering media and there influence on the seismic wave field. A systematic study of a large number of scenarios computed by highly accurate simulation methods to provide reliable synthetic data sets is necessary to test the capabilities of currently used inversion tools. Slight changes in parameters like the source position, the source mechanism or the elastic and geometric properties of the medium can then reveal the limits of such tools and provide more precise bounds of their applicability in volcano seismology.

Finally, the implementation of the ADER-DG method is still much more expensive than other state-of-the-art implementations of existing methods. However, a fair



Simulation of Seismic Wave Propagation in Media with Complex Geometries, Figure 13

Standard partitioning of the computational domain (*left*) and an example of 4 subdomains grouped together for more efficient local time stepping



Simulation of Seismic Wave Propagation in Media with Complex Geometries, Figure 14

Snapshots of the seismic wave field after an explosive event close to the summit of Merapi volcano. The free surface topography introduces strong scattering of the waves making it extremely difficult to invert for the seismic source mechanism or the exact source location

1219 comparison between accuracy and computational cost is
1220 still a pending task. The main reason for the CPU-time dif-
1221 ference is the much larger number of tetrahedral elements
1222 than hexahedrons that have to be used to cover the same
1223 volume. Furthermore, due to the choice of the basis func-
1224 tions, the flux computations are expensive, as the matrix-
1225 matrix multiplications involved are not sparse.

1226 However, the ADER-DG method is currently imple-
1227 mented on hexahedral meshes to make fair comparisons
1228 possible. Preliminary tests show, that the change of mesh
1229 topology from tetrahedrons to hexahedrons significantly re-
1230 duces the computational cost. However, final results are
1231 subject to future investigations.

1232 Discussion and Future Directions

1233 As indicated in the introduction and highlighted in the
1234 previous sections, computational tools for wave propa-
1235 gation problems are getting increasingly sophisticated to
1236 meet the needs of current scientific problems. We are far
1237 away from simple finite-difference time schemes that are
1238 solving problems on regular grids on serial computers in

1239 which case the particular programming approach did not
1240 affect dramatically the overall performance. Today, com-
1241 petitive algorithms are results of years of partly highly pro-
1242 fessional coding. Implementations on high-performance
1243 computing hardware requires in-depth knowledge of par-
1244 allel algorithms, profiling, and many technical aspects of
1245 modern computations. To make complex scientific soft-
1246 ware available to other researchers requires implementa-
1247 tion and testing on many different (parallel) platforms.
1248 This may involve parallelization using different program-
1249 ming paradigms (e. g., the combination of OpenMP and
1250 MPI on nodes of shared memory machines), and interoper-
1251 ability on heterogeneous computational GRIDS.

1252 This has dramatic consequences particularly for young
1253 researchers in the Earth Sciences who want to use ad-
1254 vanced computational tools to model observations. While
1255 in the early days a finite-difference type algorithm could
1256 be understood, coded, implemented and tested in a few
1257 weeks, this is no longer possible. In addition, standard cur-
1258 ricula do not offer training in computational methods al-
1259 lowing them to efficiently write and test codes. This sug-
1260 gests that at least for some, well-defined computational

1261 problems verified and professionally engineered scientific
 1262 software solutions should be provided to the commu-
 1263 nity and also professionally extended and maintained in
 1264 close collaboration with scientists. In seismology we are
 1265 in a quite fortunate situation. In contrast to many other
 1266 fields of physical sciences, our constitutive relations (e. g.,
 1267 stress-strain) are fairly well understood, and – as indicated
 1268 in this paper – numerical solutions for 3D problems and
 1269 their implementation on parallel hardware are well ad-
 1270 vanced. Another argument for stable tested “community”-
 1271 codes for wave propagation is the fact that advancement in
 1272 many scientific problems (e. g., imaging the Earth’s inter-
 1273 rior, quantifying earthquake-induced shaking hazard) re-
 1274 lies on zillions of forward modeling runs with only slight
 1275 variations of the internal velocity models.

1276 As far as technical developments are concerned, the
 1277 efficient initialization of complex 3D models on com-
 1278 putational grids is still a great challenge. Realistic mod-
 1279 els may be composed of complex topography, families
 1280 of overlapping fault surfaces, discontinuous interfaces,
 1281 and varying rheologies (e. g., elastic, anisotropic, viscoelas-
 1282 tic, viscoplastic, porous). This may require the combina-
 1283 tion of tetrahedral and hexahedral grid in models with
 1284 strongly varying degree of complexity. Ideally, standards
 1285 for Earth models (as well as synthetic data) formats should
 1286 be established by the communities that allow easy ex-
 1287 change and multiple use of models with different simu-
 1288 lation tools (e. g., wave propagation, deformation, earth-
 1289 quake rupture). In addition, the rapid developments to-
 1290 wards PetaFlop computing opens new questions about the
 1291 scalability and efficient parallelization of current and fu-
 1292 ture algorithms.

1293 As the forward problem of wave propagation is at the
 1294 core of the seismic imaging problem for both source and
 1295 Earth’s structure, in the near future we will see the in-
 1296 corporation of 3D simulation technology into the imag-
 1297 ing process. Provided that the background seismic velocity
 1298 models are fairly well known (e. g., reservoirs, global Earth,
 1299 sedimentary basins), adjoint methods provide a power-
 1300 ful analytical tool to (1) relate model deficiencies to misfit
 1301 in observations and (2) quantify the sensitivities to spe-
 1302 cific aspects of the observations (e. g., [100,104,105]). As
 1303 the core of the **adjoint calculations** is the seismic forward
 1304 problem, the challenge is the actual application to real data
 1305 and the appropriate parametrizations of model and data
 1306 that optimize the data fitting process.

1307 In summary, while we look back at (and forward
 1308 to) exciting developments in computational seismology,
 1309 a paradigm shift in the conception of one of the central
 1310 tools of seismology – the calculation of 3D synthetic seis-
 1311 mograms – is necessary. To extract a maximum amount of

information from our high-quality observations scientists
 should have access to high-quality simulation tools. It is
 time to accept that “*software is infrastructure*” and provide
 the means to professionally develop and maintain commu-
 nity codes and model libraries at least for basic Earth sci-
 ence problems and specific focus regions. Developments
 are one the way along those lines in the SPICE project
 (Seismic Wave Propagation and Imaging in Complex Me-
 dia, a European Network [101]), the Southern Califor-
 nia Earthquake Center (SCEC [94]) and the CIG Project
 (Computational infrastructure in geodynamics [17]).

Acknowledgments

We would like to acknowledge partial support towards this
 research from: The European Human Resources and Mo-
 bility Program (SPICE-Network), the German Research
 Foundation (Emmy Noether-Programme), the Bavarian
 Government (KOHNIHR, graduate college THESIS,
 BaCaTec), and MunichRe. We would also like to thank J.
 Tromp supporting MS’s visit to CalTech. We also thank
 two anonymous reviewers for constructive comments on
 the manuscript.

Bibliography

Primary Literature

1. Alterman Z, Karal FC (1968) Propagation of elastic waves in layered media by finite-difference methods. *Bull Seism Soc Am* 58:367–398
2. Benzley SE, Harris NJ, Scott M, Borden M, Owen SJ (2005) Conformal refinement and coarsening of unstructured hexahedral meshes. *J Comput Inf Sci Eng* 5:330–337
3. Bey J (1995) Tetrahedral grid refinement. *Computing* 55:355–378
4. Bielak J, Loukakis K, Hisada Y, Yoshimura C (2003) Domain reduction method for three-dimensional earthquake modeling in localized regions, Part I: Theory. *Bull Seism Soc Am* 93:817–824
5. Bonilla LF, Archuleta RJ, Lavallée D (2005) Hysteretic and dilatant behavior of cohesionless soils and their effects on nonlinear site response: Field data observations and modelling. *Bull Seism Soc Am* 95(6):2373–2395
6. Boore D (1972) Finite-difference methods for seismic wave propagation in heterogeneous materials. In: Bolt BA (ed) *Methods in Computational Physics*, vol 11. Academic Press, New York
7. Braun J, Sambridge MS (1995) A numerical method for solving partial differential equations on highly irregular evolving grids. *Nature* 376:655–660
8. Bunge HP, Tromp J (2003) Supercomputing moves to universities and makes possible new ways to organize computational research. *EOS* 84(4):30, 33
9. Carcione JM, Wang J-P (1993) A Chebyshev collocation method for the elastodynamic equation in generalised coordinates. *Comp Fluid Dyn* 2:269–290

- 1364 10. Carcione JM, Kosloff D, Kosloff R (1988) Viscoacoustic wave
1365 propagation simulation in the earth. *Geophysics* 53:769–777
1366 11. Carcione JM, Kosloff D, Behle A, Seriani G (1992) A spec-
1367 tral scheme for wave propagation simulation in 3-D elastic-
1368 anisotropic media. *Geophysics* 57:1593–1607
1369 12. Carey G (1997) *Computational grids: Generation, adaptation,
1370 and solution strategies*. Taylor Francis, New York
1371 13. Cerveny V (2001) *Seismic ray theory*. Cambridge University
1372 Press, Cambridge
1373 14. Chaljub E, Tarantola A (1997) Sensitivity of SS precursors to
1374 topography on the upper-mantle 660-km discontinuity. *Geophy-
1375 s Res Lett* 24(21):2613–2616
1376 15. Chaljub E, Komatitsch D, Vilotte JP, Capdeville Y, Valette B,
1377 Festa G (2007) Spectral element analysis in seismology. In:
1378 Wu R-S, Maupin V (eds) *Advances in wave propagation in hetero-
1379 geneous media*. *Advances in Geophysics*, vol 48. Elsevier,
1380 **TS7**, pp 365–419
1381 16. Chapman CH (2004) *Fundamentals of seismic wave propaga-
1382 tion*. Cambridge University Press, Cambridge
1383 17. CIG www.geodynamics.org **TS9**
1384 18. Cockburn B, Shu CW (1989) TVB Runge–Kutta local projection
1385 discontinuous Galerkin finite element method for conserva-
1386 tion laws II: General framework. *Math Comp* 52:411–435
1387 19. Cockburn B, Shu CW (1991) The Runge–Kutta local projection
1388 P1-Discontinuous Galerkin finite element method for scalar
1389 conservation laws. *Math Model Numer Anal* 25:337–361
1390 20. Cockburn B, Shu CW (1998) The Runge–Kutta discontinuous
1391 Galerkin method for conservation laws V: Multidimensional
1392 systems. *J Comput Phys* 141:199–224
1393 21. Cockburn B, Lin SY, Shu CW (1989) TVB Runge–Kutta local
1394 projection discontinuous Galerkin finite element method for
1395 conservation laws III: One dimensional systems. *J Comput
1396 Phys* 84:90–113
1397 22. Cockburn B, Hou S, Shu CW (1990) The Runge–Kutta local
1398 projection discontinuous Galerkin finite element method for
1399 conservation laws IV: The multidimensional case. *Math Comp*
1400 54:545–581
1401 23. Cockburn B, Karniadakis GE, Shu CW (2000) Discontinuous
1402 Galerkin methods, theory, computation and applications.
1403 *LNCSE*, vol 11. Springer, New York
1404 24. Courant R, Friedrichs KO, Lewy H (1928) Über die partiellen
1405 Differenzialgleichungen der **TS8**
1406 25. CUBIT cubit.sandia.gov **TS9**
1407 26. Dablain MA (1986) The application of high-order differencing to
1408 the scalar wave equation. *Geophysics* 51:54–66
1409 27. De Cougny HL, Shephard MS (1999) Parallel refinement and
1410 coarsening of tetrahedral meshes. *Int J Numer Methods Eng*
1411 46:1101–1125
1412 28. de la Puente J, Dumbser M, Käser M, Igel H (2007) Discontin-
1413 uous Galerkin methods for wave propagation in poroelastic
1414 media (submitted) **TS10**
1415 29. de la Puente J, Käser M, Dumbser M, Igel H (2007) An arbi-
1416 trary high order discontinuous Galerkin method for elastic
1417 waves on unstructured meshes IV: Anisotropy. *Geophys J Int*
1418 169(3):1210–1228
1419 30. di Prisco C, Stupazzini M, Zambelli C (2007) Non-linear SEM
1420 numerical analyses of dry dense sand specimens under rapid
1421 and dynamic loading. *Int J Numer Anal Methods Geomech*
1422 31(6):757–788
31. Dormy E, Tarantola A (1995) Numerical simulation of elastic 1423
wave propagation using a finite volume method. *J Geophys* 1424
Res 100(B2):2123–2134 1425
32. Dumbser M (2005) Arbitrary high order schemes for the solu- 1426
tion of hyperbolic conservation laws in complex domains. 1427
Shaker, Aachen 1428
33. Dumbser M, Käser M (2006) An arbitrary high order discon- 1429
tinuous galerkin method for elastic waves on unstructured 1430
meshes II: The three-dimensional isotropic case. *Geophys J Int* 1431
167:319–336 1432
34. Dumbser M, Käser M (2007) Arbitrary high order non-oscilla- 1433
tory finite volume schemes on unstructured meshes for lin- 1434
ear hyperbolic systems. *J Comput Phys* 221:693–723. doi:10. 1435
1016/j.jcp.2006.06.043 1436
35. Dumbser M, Munz CD (2005) Arbitrary high order discontinu- 1437
ous Galerkin schemes. In: Cordier S, Goudon T, Gutnic M, Son- 1438
nendrucker E (eds) *Numerical methods for hyperbolic and kin- 1439
etic problems*. IRMA series in mathematics and theoretical
1440 physics. EMS Publishing, Zurich, pp 295–333 1441
36. Dumbser M, Käser M, Toro EF (2007) An arbitrary high-order 1442
discontinuous Galerkin method for elastic waves on unstruc- 1443
tured meshes – V. Local time stepping and p-adaptivity. *Geophy- 1444
s J Int (in press)* **TS10** 1445
37. Dziewonski AM, Anderson DL (1981) Preliminary reference 1446
earth model. *Phys Earth Planet Inter* 25:297–356 1447
38. Ewald M, Igel H, Hinzen K-G, Scherbaum F (2006) Basin-re- 1448
lated effects on ground motion for earthquake scenarios in 1449
the lower rhine embayment. *Geophys J Int* 166:197–212 1450
39. Faccioli E, Maggio F, Quarteroni A, Tagliani A (1996) Spectral- 1451
domain decomposition methods for the solution of acoustic 1452
and elastic wave equation. *Geophysics* 61:1160–1174 1453
40. Faccioli E, Maggio F, Paolucci R, Quarteroni A (1997) 2D and 1454
3D elastic wave propagation by a pseudo-spectral domain 1455
decomposition method. *J Seismol* 1:237–251 1456
41. Faccioli E, Vanini M, Paolucci R, Stupazzini M (2005) Comment 1457
on “Domain reduction method for three-dimensional earth- 1458
quake modeling in localized regions, part I: Theory.” by Bielak 1459
J, Loukakis K, Hisada Y, Yoshimura C, and “Part II: Verification 1460
and Applications.” by Yoshimura C, Bielak J, Hisada Y, Fernán- 1461
dez A. *Bull Seism Soc Am* 95:763–769 1462
42. Falk J, Tessmer E, Gajewski D (1996) Efficient finite-difference 1463
modelling of seismic waves using locally adjustable time 1464
steps. *Geophys Prosp* 46:603–616 1465
43. Falk J, Tessmer E, Gajewski D (1996) Tube wave modelling by 1466
the finite differences method with varying grid spacing. *Pure
Appl Geoph* 148:77–93 1467
44. Fernandez A, Bielak J, Prentice C (2006) Urban seismology; 1469
City effects on earthquake ground motion and effects of 1470
spatial distribution of ground motion on structural response 1471
paper presented at 2006 annual meeting. *Seism Res Lett*
1472 77(2):305 1473
45. Fornberg B (1996) *A practical guide to pseudospectral meth-
1474 ods*. Cambridge University Press, Cambridge 1475
46. Fuchs K, Müller G (1971) Computation of synthetic seismo- 1476
grams with the reflectivity method and comparison with ob- 1477
servations. *Geophys J Royal Astronom Soc* 23(4):417–33 1478
47. Furumura T, Takenaka H (1996) 2.5-D modeling of elastic 1479
waves using the pseudospectral method. *Geophys J Int* 124: 1480
820–832 1481

TS7 Please supply publisher location.

TS8 Please complete this reference.

TS9 Please supply access date.

TS10 Please update if possible.

- 1482 48. Geller RJ, Takeuchi N (1998) Optimally accurate second-order
1483 time-domain finite difference scheme for the elastic equation
1484 of motion: One-dimensional case. *Geophys J Int* 135:48–62
1485 49. Graves RW (1993) Modeling three-dimensional site response
1486 effects in the Marina district basin, San Francisco, California.
1487 *Bull Seism Soc Am* 83:1042–1063
1488 50. Hestholm SO, Ruud BO (1998) 3-D finite-difference elastic
1489 wave modeling including surface topography. *Geophysics*
1490 63:613–622
1491 51. Holberg O (1987) Computational aspects of the choice of
1492 operator and sampling interval for numerical differentia-
1493 tion in large-scale simulation of wave phenomena. *Geophys*
1494 *Prospect* 35:629–655
1495 52. Igel H (1999) Wave propagation through 3-D spherical sec-
1496 tions using the Chebyshev spectral method. *Geop J Int*
1497 136:559–567
1498 53. Igel H, Gudmundsson O (1997) Frequency-dependent ef-
1499 fects on travel times and waveforms of long-period S and SS
1500 waves. *Phys Earth Planet Inter* 104:229–246
1501 54. Igel H, Weber M (1995) SH-wave propagation in the whole
1502 mantle using high-order finite differences. *Geophys Res Lett*
1503 22(6):731–734
1504 55. Igel H, Weber M (1996) P-SV wave propagation in the Earth's
1505 mantle using finite-differences: Application to heteroge-
1506 neous lowermost mantle structure. *Geophys Res Lett* 23:415–
1507 418
1508 56. Igel H, Mora P, Rioulet B (1995) Anisotropic wave propagation
1509 through finite-difference grids. *Geophysics* 60:1203–1216
1510 57. Igel H, Nissen-Meyer T, Jahnke G (2001) Wave propagation
1511 in 3-D spherical sections: Effects of subduction zones. *Phys*
1512 *Earth Planet Inter* 132:219–234
1513 58. Jahnke G, Igel H, Cochard A, Thorne M (2007) Parallel imple-
1514 mentation of axisymmetric SH wave propagation in spherical
1515 geometry. *Geophys J Int* (in print) **TS10**
1516 59. Jastram C, Tessmer E (1994) Elastic modelling on a grid with
1517 vertically varying spacing. *Geophys Prosp* 42:357–370
1518 60. Karypis G, Kumar V (1998) Multilevel k-way Partitioning
1519 Scheme for Irregular Graphs. *J Parallel Distrib Comput*
1520 48(1):96–129
1521 61. Kelly KR, Ward RW, Treitel S, Alford RM (1976) Synthetic seis-
1522 mograms: A finite-difference approach. *Geophysics* 41:2–27
1523 62. Kennett BLN (2002) *The seismic wavefield, vol I + II*. Cam-
1524 bridge University Press, Cambridge
1525 63. Komatitsch D, Tromp J (2002) Spectral-element simulations
1526 of global seismic wave propagation, part I: Validation. *Geo-*
1527 *phys J Int* 149:390–412
1528 64. Komatitsch D, Tromp J (2002) Spectral-element simulations
1529 of global seismic wave propagation, part II: 3-D models,
1530 oceans, rotation, and gravity. *Geophys J Int* 150:303–318
1531 65. Komatitsch D, Vilotte JP (1998) The spectral-element method:
1532 An efficient tool to simulate the seismic response of 2D and
1533 3D geological structures. *Bull Seism Soc Am* 88:368–392
1534 66. Komatitsch D, Coutel F, Mora P (1996) Tensorial formulation
1535 of the wave equation for modelling curved interfaces. *Geo-*
1536 *phys J Int* 127(1):156–168
1537 67. Kosloff DD, Baysal E (1982) Forward modeling by a fourier
1538 method. *Geophysics* 47(10):1402–1412
1539 68. Krishnan S, Ji C, Komatitsch D, Tromp J (2006) Case studies
1540 of damage to tall steel moment-frame buildings in Southern
1541 California during large San Andreas earthquakes. *Bull Seismol*
1542 *Soc Am* 96(4A):1523–1537
69. Krishnan S, Ji C, Komatitsch D, Tromp J (2006) Performance of
1543 two 18-story steel moment-frame buildings in Southern Cal-
1544 ifornia during two large simulated San Andreas earthquakes.
1545 *Earthq Spectra* 22(4):1035–106
1546 70. Käser M, Dumbser M (2006) An arbitrary high order discon-
1547 tinuous Galerkin method for elastic waves on unstructured
1548 meshes I: The two-dimensional isotropic case with external
1549 source terms. *Geophys J Int* 166:855–877
1550 71. Käser M, Dumbser M, de la Puente J, Igel H (2007) An arbitrary
1551 high order discontinuous Galerkin method for elastic waves
1552 on unstructured meshes III: Viscoelastic attenuation. *Geophys*
1553 *J Int* 168(1):224–242
1554 72. Käser M, Igel H (2001) Numerical simulation of 2D wave prop-
1555 agation on unstructured grids using explicit differential oper-
1556 ators. *Geophys Prospect* 49(5):607–619
1557 73. Käser M, Igel H, Sambridge M, Braun J (2001) A compara-
1558 tive study of explicit differential operators on arbitrary grids.
1559 *J Comput Acoust* 9(3):1111–1125
1560 74. Kwak D-Y, Im Y-T (2002) Remeshing for metal forming simu-
1561 lations – part II: Three dimensional hexahedral mesh genera-
1562 tion. *Int J Numer Methods Eng* 53:2501–2528
1563 75. LeVeque RL (2002) *Finite volume methods for hyperbolic*
1564 *problems*. Cambridge University Press, Cambridge
1565 76. Levander AR (1988) Fourth-order finite-difference P-SV seis-
1566 mograms. *Geophysics* 53:1425–1436
1567 77. Madariaga R (1976) Dynamics of an expanding circular fault.
1568 *Bull Seismol Soc Am* 66(3):639–66
1569 78. Magnier S-A, Mora P, Tarantola A (1994) Finite differences on
1570 minimal grids. *Geophysics* 59:1435–1443
1571 79. Marfurt KJ (1984) Accuracy of finite-difference and finite-ele-
1572 ment modeling of the scalar and elastic wave equations. *Geo-*
1573 *physics* 49:533–549
1574 80. Mercier ED, Vilotte JP, Sanchez-Sesma FJ (2006) Triangu-
1575 lar spectral element simulation of two-dimensional elastic
1576 wave propagation using unstructured triangular grids. *Geo-*
1577 *phys J Int* 166(2):679–698
1578 81. METIS glaros.dtc.umn.edu/gkhome/views/metis **TS9**
1579 82. Moczo P (1989) Finite-difference techniques for SH-waves in
1580 2-D media using irregular grids – Application to the seismic
1581 response problem. *Geophys J Int* 99:321–329
1582 83. Moczo P, Kristek J, Halada L (2000) 3D 4th-order staggered
1583 grid finite-difference schemes: Stability and grid dispersion.
1584 *Bull Seism Soc Am* 90:587–603
1585 84. Montelli R, Nolet G, Dahlen FA, Masters G, Engdahl ER, Hung
1586 S (2004) Finite-frequency tomography reveals a variety of
1587 plumes in the mantle. *Science* 303(5656):338–343
1588 85. Müller G (1977) Earth-flattening approximation for body
1589 waves derived from geometric ray theory – improvements,
1590 corrections and range of applicability. *J Geophys* 42:429–436
1591 86. Nissen-Meyer T, Fournier A, Dahlen FA (2007) A 2-D
1592 spectral-element method for computing spherical-earth seis-
1593 mograms – I. Moment-tensor source. *Geophys J Int* (in
1594 press) **TS10**
1595 87. Ohminato T, Chouet BA (1997) A free-surface boundary con-
1596 dition for including 3D topography in the finite-difference
1597 method. *Bull Seism Soc Am* 87:494–515
1598 88. Oprašal I, J Zahradník (1999) Elastic finite-difference method
1599 for irregular grids. *Geophysics* 64:240–250
1600 89. Pitarka A (1999) 3D elastic finite-difference modeling of seis-
1601 mic motion using staggered grids with nonuniform spacing.
1602 *Bull Seism Soc Am* 89:54–68
1603

- 1604 90. Priolo E, Carcione JM, Seriani G (1996) Numerical simulation of
1605 interface waves by high-order spectral modeling techniques.
1606 *J Acoust Soc Am* 95:681–693
- 1607 91. Reed WH, Hill TR (1973) Triangular mesh methods for the neu-
1608 tron transport equation. Technical Report, LA-UR-73-479, Los
1609 Alamos Scientific Laboratory
- 1610 92. Ripperger J, Igel H, Wassermann J (2004) Seismic wave simu-
1611 lation in the presence of real volcano topography. *J Volcanol*
1612 *Geotherm Res* 128:31–44
- 1613 93. Scandella L (2007) Numerical evaluation of transient ground
1614 strains for the seismic response analyses of underground
1615 structures. PhD. Thesis, Milan University of Technology, Milan
- 1616 94. SCEC www.scec.org **TS9**
- 1617 95. Schneiders R (2000) Octree-Based Hexahedral Mesh Genera-
1618 tion. *Int J Comput Geom Appl* 10(4):383–398
- 1619 96. Schwartzkopff T, Munz CD, Toro EF (2002) ADER: A high-order
1620 approach for linear hyperbolic systems in 2D. *J Sci Comput*
1621 17:231–240
- 1622 97. Schwartzkopff T, Dumbser M, Munz CD (2004) Fast high or-
1623 der ADER schemes for linear hyperbolic equations. *J Comput*
1624 *Phys* 197:532–539
- 1625 98. Seriani G, Priolo E, Carcione JM, Padovani E (1992) High-order
1626 spectral element method for elastic wave modeling: 62nd
1627 *Ann. Internat. Mtg., Soc. Expl. Geophys., Expanded Abstracts,*
1628 1285–1288
- 1629 99. Shepherd JF (2007) Topologic and geometric constraint-
1630 based hexahedral mesh generation. PhD. Thesis on Com-
1631 puter Science, School of Computing The University of Utah,
1632 **TS7**
- 1633 100. Sieminski A, Liu Q, Trampert J, Tromp J (2007) Finite-fre-
1634 quency sensitivity of surface waves to anisotropy based upon
1635 adjoint methods. *Geophys J Int* (in press) **TS10**
- 1636 101. SPICE www.spice-rtn.org **TS9**
- 1637 102. Stupazzini M (2004) A spectral element approach for 3D dy-
1638 namic soil-structure interaction problems. PhD. Thesis, Milan
1639 University of Technology, Milan
- 1640 103. Takeuchi N, Geller RJ (2000) Optimally accurate second or-
1641 der time-domain finite difference scheme for computing syn-
1642 thetic seismograms in 2-D and 3-D media. *Phys Earth Planet*
1643 *Int* 119:99–131
- 1644 104. Tape C, Liu Q, Tromp J (2007) Finite-frequency tomography
1645 using adjoint methods: Methodology and examples using
1646 membrane surface waves. *Geophys J Int* 168:1105–1129
- 1647 105. Tarantola A (1986) A strategy for nonlinear elastic inversion of
1648 seismic reflection data. *Geophysics* 51(10):1893–1903
- 1649 106. Tessmer E (2000) Seismic finite-difference modeling with spa-
1650 tially varying time steps. *Geophysics* 65:1290–1293
- 1651 107. Tessmer K, Kosloff D (1996) 3-D elastic modeling with surface
1652 topography by a Chebychev spectral method. *Geophysics*
1653 59:464–473
- 1654 108. Tessmer E, Kessler D, Kosloff K, Behle A (1996) Multi-domain
1655 Chebyshev–Fourier method for the solution of the equations
1656 of motion of dynamic elasticity. *J Comput Phys* 100:355–363
- 1657 109. Thomas C, Igel H, Weber M, Scherbaum F (2000) Acoustic simu-
1658 lation of P-wave propagation in a heterogeneous spherical
1659 earth: Numerical method and application to precursor energy
1660 to PKPdf. *Geophys J Int* 141:307–320
- 1661 110. Thorne M, Lay T, Garnero E, Jahnke G, Igel H (2007) 3-D seis-
1662 mic imaging of the D'' region beneath the Cocos Plate. *Geophys J Int* (in print) **TS10**
111. Titarev VA, Toro EF (2002) ADER: Arbitrary high order Go-
1664 dunov approach. *J Sci Comput* 17:609–618 1665
112. Toro EF (1999) Riemann solvers and numerical methods for
1666 fluid dynamics. Springer, Berlin 1667
113. Toro EF, Millington AC, Nejad LA (2001) Towards very high
1668 order Godunov schemes, in *Godunov methods; Theory and*
1669 *applications*. Kluwer/Plenum, Oxford, pp 907–940 1670
114. Toyokuni G, Takenaka H, Wang Y, Kennett BLN (2005) Quasi-
1671 spherical approach for seismic wave modeling in a 2-D slice
1672 of a global earth model with lateral heterogeneity. *Geophys*
1673 *Res Lett* 32:L09305 **TS11** 1674
115. Van der Hilst RD (2004) Changing views on Earth’s deep man-
1675 tle. *Science* 306:817–818 1676
116. Virieux J (1984) SH-wave propagation in heterogeneous
1677 media: Velocity-stress finite-difference method. *Geophysics*
1678 49:1933–1957 1679
117. Virieux J (1986) P-SV wave propagation in heterogeneous
1680 media: Velocity-stress finite-difference method. *Geophysics*
1681 51:889–901 1682
118. Woodhouse JH, Dziewonski AM (1984) Mapping the upper
1683 mantle: Three dimensional modelling of earth structure by in-
1684 version of seismic waveforms. *J Geophys Res* 89:5953–5986 1685
119. Yoshimura C, Bielak J, Hisada Y, Fernández A (2003) Domain
1686 reduction method for three-dimensional earthquake model-
1687 ing in localized regions, part II: Verification and applications.
1688 *Bull Seism Soc Am* 93:825–841 1689
120. Zambelli C (2006) Experimental and theoretical analysis of the
1690 mechanical behaviour of cohesionless soils under cyclic-dy-
1691 namic loading. PhD. Thesis, Milan University of Technology,
1692 Milan 1693
121. Zienkiewicz O, Taylor RL (1989) *The finite element method,*
1694 *vol 1*. McGraw-Hill, London 1695

Books and Reviews

- Carcione JM, Herman GC, ten Kroode APE (2002) Seismic mod-
1696 elling. *Geophysics* 67:1304–1325 1697
- Mozco P, Kristek J, Halada L (2004) *The finite-difference method*
1698 *for seismologists: An introduction*. Comenius University,
1699 Bratislava. Available in pdf format at [ftp://ftp.nuquake.eu/](ftp://ftp.nuquake.eu/pub/Papers)
1700 [pub/Papers](ftp://ftp.nuquake.eu/pub/Papers) 1701
- Mozco P, Kristek J, Galis M, Pazak P, Balazovjeh M (2007) The fi-
1702 nite difference and finite-element modelling of seismic wave
1703 propagation and earthquake motion. *Acta Physica Slovaca,*
1704 57(2) **TS12** 1705
- Wu RS, Maupin V (eds) (2006) *Advances in wave propagation in*
1706 *heterogeneous earth*. In: Dmowska R (ed) *Advances in geo-*
1707 *physics, vol 48*. Academic/Elsevier, **TS7** 1708

TS11 Please check. Is this correct?

TS12 Please supply page(s).